Evidence For Active Tectonics Along The Australian Passive Margin: Quaternary Marine Terraces Of Waratah Bay, Victoria

Terri Ann Amborn
Department of Geological Sciences
California Polytechnic University, Pomona
2003

California State Polytechnic University, Pomona

Abstract

EVIDENCE FOR ACTIVE TECTONICS ALONG THE AUSTRALIAN PASSIVE MARGIN: QUATERNARY MARINE TERRACES OF WARATAH BAY, VICTORIA

by Terri Ann Amborn

Thesis Advisor: Jeffrey S. Marshall
Geological Sciences Department

Located within the interior of the Australian-Indian plate, the continental margin of Australia is generally described as a classic passive margin. However, along the southeastern coast, historical seismicity and a variety of anomalous geologic and geomorphic features indicate active crustal deformation. At Waratah Bay, Victoria, a prominent flight of at least six uplifted marine terraces wraps around the rocky headland of Cape Liptrap and extends northeastward toward the Yanakie isthmus inland of Wilson's Promontory. Wave-cut platforms developed across Paleozoic marine sedimentary bedrock are covered by Quaternary deposits of silicic beach and dune sands, angular quartz gravels, and estuarine silt and clay horizons. The spatial distribution of the terraces was defined through field mapping, aerial photo analysis, and GPS surveying. A series of topographic profiles surveyed across the terraces show that tread elevations decrease toward the northeast away from Cape Liptrap. Uplift and tilting of these terraces may reflect Quaternary slip along the NE trending Waratah Fault. Active crustal deformation in this region may result from denudation and isostatic flexure, variations in the crust/mantle thermal structure, and/or far-field intraplate stresses.

TABLE OF CONTENTS

LIST OF FIGURES AND TABLES

FIGURES

TABLES

Evidence for Active Tectonics Along the Australian Passive Margin: Quaternary Marine Terraces of Waratah Bay, Victoria.

by Terri Ann Amborn
Thesis Advisor: Jeffrey S. Marshall, Geological Sciences Department, Cal Poly Pomona.

Introduction

Located within the interior of the Australian-Indian Plate, the continental margin of Australia is generally described as a classic passive margin (Fig.1). However, along the southeastern coast, historical seismicity and a variety of anomalous geologic and geomorphic features indicate active crustal deformation (Gibson et al, 1981; Abele, 1988; Jenkin, 1988; Ollier and Pain, 1994). Southeast Australia is known for such dramatic topographic features as the Great Escarpment and the Australian highlands. Late Cenozoic faulting is associated with both features and, at some localities, Paleozoic rocks have been thrust over Quaternary gravels (Orr, 1998). Offset Neogene to Quaternary fluvial deposits, marine terraces, and aeolian sands have also been cited as evidence for ongoing tectonism in the region (Gardner, 2003).

This study investigates geomorphic evidence for active tectonism along a segment of the southeastern Australian coast at Waratah Bay, Victoria (Fig. 2). Here, a flight of Late Neogene-Quaternary marine terraces wraps around the rocky headland of Cape Liptrap and extends eastward toward the Yanakie isthmus inland of Wilson's Promontory. The purpose of this study is to map these terrace surfaces, establish age constraints, and identify evidence of deformation. The results of this investigation provide new insights into the geomorphic and tectonic history of the southeastern Australian passive margin.

Geology and Tectonics of Southeast Victoria

Bassian Zone

Offshore Victoria is referred to as the Bassian Zone, a tectonic province that consists of the Bass, Otway, and Gippsland Basins, all formed during Early Cretaceous rifting between Australia and Antarctica (Abele, 1988). The Bassian Zone (Fig. 3) runs

east-west across the southern coast of Victoria and stretches south towards Tasmania. Rifting and extension between these land masses resulted in the formation of the three Bassian Zone basins (Fig. 4). Faulting in the basins includes Cretaceous normal faults, steeply dipping transfer faults, and younger Tertiary reverse faults which may be associated with northeast trending anticlines.

Gippsland Basin

Structure. The majority of the Gippsland basin (Fig. 5) is located off shore with the exception of its western fifth, which extends onland into the area of south Gippsland, Victoria (Abele, 1988). The western boundary of the basin is formed by faulted, uplifted Cretaceous blocks. The Eastern Highlands bound the basin to the north and the Bassian rise separates the Gippsland and Bass Basin to the south. The eastern margin is open to the Tasman Sea and creates the continental slope.

Normal faults of Late Cretaceous and Early Tertiary ages are better recognized offshore than onshore, a characteristic that is similar in the Bass Basin. Also similar in both basins is the northwest trend of the normal faults. In the western onland portion of the Gippsland Basin, Tertiary anticlines trend northeast and are arranged en echelon. Older and similar en echelon folds can be seen in the offshore portion of the Gippsland Basin to the east.

The 40 kilometer-long Baragwanath Anticline (Fig. 5) is the largest Tertiary fold that extends onland into South Gippsland (Abele, 1988). At the surface, it forms a long ridge with topographic relief of 210 meters (Jenkin, 1968). Normal faults are also present in this area. These structures generally merge along strike into monoclines with unfaulted beds draped over a buried fault. Late Tertiary thrust faults also occur in the onshore portion of the Gippsland Basin, and are responsible for placing older basalt flows of the Latrobe Valley Group over younger coal beds.

Stratigraphy. A major transgressive-regressive cycle can be seen in the stratigraphy of the Gippsland basin (Abele, 1988). Early Cretaceous deposits are covered by a 6000 meter thick section of Late Cretaceous to Recent sediments and volcanic rocks. The Early Tertiary Latrobe Valley Group, made up of continental clastic sediments, coal

beds, and volcanics, makes up a major portion of these deposits. Near the northwest margin of the basin, coal seams of the Latrobe Valley Group are overlain unconformably by Pliocene and younger sediment. The rest of the basin is unconformably overlain by up to 1800 meters of calcareous limestones, marls, marine limestones, and sandstones, which make up the Seaspray Group. The onshore part of the Gippsland basin is blanketed by the Miocene to Pliocene Sale Group, including marine sands, silts, and clays.

Tectonics. During Cretaceous rifting, subsidence occurred in Gippsland, while uplift gave rise to the Eastern Highlands (Abele, 1988). During the Early Tertiary, upwarping triggered volcanism in southeast Gippsland. Much of the volcanics were eroded before the deposition of the Latrobe Valley Group occurred. During the Early Miocene, renewed subsidence caused partial submergence of southeast Gippsland followed by regression during the Late Miocene, and a marine environment again in the Early Pliocene. Swamp and lake deposition occurred during this time, while upwarping in the north and subsidence in the east occurred. The effects of warping during the Pleistocene can be seen in the following ways: tilted marine terraces, submerged terrestrial deposits, swamp formation in tectonic depressions, and offset of Pliocene sediments, including the Haunted Hill Gravels (Jenkin, 1968).

Seismicity. Australia is a seismically active continent (Fig. 6), with much activity focused in the southeast (Sandiford, 2002). Up until 1840, there were no data collected on Victorian earthquakes. The first seismograph was established in Melbourne in 1888. This instrument did not easily detect higher frequencies, making earthquakes difficult to locate accurately (Gibson et al., 1981). Before 1960, earthquake epicenters were generally chosen as the locations with the highest ground shaking intensities. Melbourne was thought to be the location of the majority of earthquake epicenters because it was highly populated, and therefore, had more intensity reports.

By 1981, 11 seismographs were added to Victoria (Gibson et al, 1981). Since then, the Seismology Research Center (SRC) has developed a network of seismographs totaling over 80 which can be found across Victoria and New South Wales. The SRC records an average of 400 earthquakes a year (half of them magnitude 3 or greater).

Epicenters are generally located along Cretaceous-Tertiary age structures thought to have been reactivated during the Late Cenozoic.

Geomorphology of South Gippsland

Wilson's Promontory and Yanakie Isthmus

Wilson's Promontory extends over 40 kilometers into the Bass Strait marking the southern most tip of the Australian mainland (Figs. 2 & 3). The Promontory consists of a major batholith of Devonian granites supporting a mountain range with elevations reaching over 700 meters above sea level. A granite belt extends from the east coast of Tasmania across the Bass Strait, with the northern end being Wilson's Promontory batholith. About 600 square kilometers of granite is exposed, while another 600 square kilometers of granite is submerged, or covered with swamp and dune deposits. The many different types of granite that make up the batholith occur in seven zones: Glennie granite, Biotite granite, Pale granite, Xenolith granite, Porphyritic granite, Sealers granite, and Singapore granite (Abele, 1988). The Wilson's Promontory granites are very susceptible to weathering, providing a source of sediment for the beaches, dunes, and the Yanakie isthmus, a sedimentary lowland connecting the promontory with the Gippsland Highlands, to the north (Fig. 2).

Vertical faults are responsible for the current shape of Wilson's Promontory. Faulting during the Cretaceous contributed to erosion of the granite, which was gradually deposited into the Gippsland Basin. Erosion along the faults created valleys, and is also responsible for removing a thick overburden of weathered granite debris revealing rounded boulder tors. Caves caused by marine erosion are seen above present day sea levels indicating sea level was once higher in this area.

Quaternary sediments occur in various forms at Wilson's Promontory. Fluvial deposits from streams draining the Wilson's promontory batholith consist of quartz sands and clays with abundant feldspar clasts and granitic lithic fragments. Colluvial material along the slopes of the granitic mountains consist of landslide, rockfall, and creep deposits. Extensive dune complexes occur along the coast of Wilson's Promontory as well as on the adjacent Yanakie isthmus. Siliceous sands occur primarily on the east side

of Wilson's Promontory while the calcareous sands are restricted to the west side. Multiple phases of dune formation have been linked to arid periods with increased wind strength associated with Pleistocene glaciation (Tuddenham, 1970). During sea level low stands, Tasmania and Wilson's Promontory were connected via the Bassian Rise (Fig. 3). Wilson's Promontory was last an island over 100,000 years ago (Mosely, 2002).

Haunted Hill Gravels

The Haunted Hill Formation consists of widely dispersed deposits of coarse grained silicic sediments which overlie Tertiary aged and older units throughout southeast Victoria (Hocking et al., 1988; Bolger, 1991). On the Yanakie Isthmus, these gravel deposits mantle the low-relief landscape surface between Wilson's Promontory and the mainland (Fig. 2). The gravels were deposited during the Pliocene and were partially eroded and redeposited during Late Pleistocene (Bolger,1991; Bremer, 2003). The formation has a wide range in particle size, and is poorly sorted. This unit varies in lithology from clay lenses to cross-bedded, angular, quartz sands and gravels, to massive boulder beds. The thickness of the gravel beds averages 12-15 meters and reaches a maximum of 30 meters. The thickest beds are comprised of clay and sand units interbedded with the gravels. Oxidation within the gravels is common resulting in orange-yellow staining. The sources of the quartz gravels are quartz veins in the Lower Devonian Liptrap Formation and from Upper Devonian granite of Wilson's Promontory (Bremer, 2003).

Corner Inlet

Corner Inlet is located between Wilson's Promontory, Yanakie isthmus and the Gippsland mainland (Fig. 2). This major estuary consists of a complex network of mangroves, mud banks, salt marshes, sea grass beds, rocky islands, deep channels, and over 40 barrier islands including Snake Island, the largest sand island in Victoria. These barrier islands protect the Inlet's mangroves, intertidal mudflats, and other estuarine habitats from the energetic waves of the Bass Strait. A smaller inlet on Waratah Bay to the west, referred to as Shallow Inlet, forms a tidal embayment that is separated from the

ocean by sand spits, sand bars, and mobile dunes. The western side of Shallow Inlet is dominated by salt marshes.

Cape Liptrap and Waratah Bay

Cape Liptrap consists of a rocky headland located to the west of Wilson's Promontory (Fig. 2). The broad embayment between these two prominent headlands is referred to as Waratah Bay. The coastline of Cape Liptrap is rugged and cliff faces are actively eroding into Lower Paleozoic marine carbonates, igneous rocks, and volcancaniclastic sediments (Hocking et al., 1988). In contrast, the north shore of Waratah Bay exhibits a depositional shoreline with a gradual increase of elevation inland. Quaternary beach, dune, and back beach comprise the shore of Waratah Bay, while thick marine sand deposits cover much of the inland area.

Tectonic Geomorphology of Cape Liptrap and Waratah Bay

Keck Geology Consortium Research Project. The Keck Geology Consortium is made up of twelve colleges within the United States that have high quality geology programs. The Consortium sponsors annual research projects to provide undergraduate students with field research and problem solving experiences. These projects are designed and directed by faculty from consortium colleges. Students chosen for the project each identify a specific problem as their research topic. The students develop a research plan, conduct background research, gather field data, analyze their data, and interpret their results. They then present the results in oral and poster presentations at the annual Keck Geology Symposium. The advanced, junior level projects for 2002 were located in Idaho, Ohio, Ireland, and Australia. This thesis is a product of the Australia project (Gardner, 2003), designed to examine evidence of Late Cenozoic tectonism at Cape Liptrap, southeast Victoria.

There were three broad topics covered on the Keck Australia Project: 1.) marine terraces 2.) aeolian deposits, and 3.) fluvial gravels. Marine terraces were examined between Cape Liptrap and the town of Waratah Bay in order to evaluate the style and magnitude of Cenozoic deformation. These features had not been mapped previously and

no data had been collected on active faulting in this area. The aeolian deposits were mapped and dated at Arch Rock and Morgan's Beach to better understand the complex history of dune formation and sea level change in that area. In addition, unusual sand concretions were examined in the aeolian deposits revealing important information on groundwater flow. Finally, the stratigraphy, sedimentology, and structure of the Haunted Hill gravels were studied to shed light on Late Cenozoic tectonism and landscape evolution in this area. Together, these individual projects provide insights into the Neogene and Quaternary geology and geomorphology of Cape Liptrap.

Waratah Bay Marine Terraces. A sequence of marine terraces was identified along the shorelines of Cape Liptrap and Waratah Bay (Gardner, 2003). Three students focused their research on these terraces (Amborn, 2003; Pezzia, 2003; Tunnell, 2003), each working in three adjacent field areas. This thesis presents results from the northeastern study area near Waratah Bay (Amborn, 2003; Amborn et al.,2003). The goal of this study was to map this terrace sequence in detail, to establish elevation and age constraints, and to identify any evidence of deformation. The results of this investigation can be used in developing new models that better explain tectonic activity observed along the eastern passive margin of Australia.

Methods

Marine Terrace Studies

Marine terraces provide significant contributions to the understanding of active tectonics in coastal areas. These broad, flat, surfaces record former shorelines along the coast (Bull, 1985; Lajoie, 1986; Anderson et al., 1999). They are created through the combined effort of fluctuating eustatic sea level and ongoing tectonic uplift.

There are three main factors that drive global sea level change through time. Sea level is controlled by changes in the form of ocean basins, change in elevation of the continental shelf relative to the ocean, and the formation or retreat of world wide glaciers. Both ocean basin size and continental shelf elevation are influenced by tectonics. Glacial advance and retreat are linked to global climate fluctuations, and have a direct effect on sea level change.

Sea level graphs for the last 500,000 years (Fig. 7) come from two main data sources: 1). Coral reef terraces on tropical coasts that have been uplifted, and 2). deviation from a standard of $^{18}O/^{16}O$ ratios in deep sea cores (Bloom and Yonekura, 1990). These two methods provide similar results when compared. The deep sea cores reveal oxygen isotope data that reflect ocean temperature changes over long periods of time. In conjunction with radiometric dating, these cores are used to track climatic changes over the past 850,000 years (Shackleton and Opdyke, 1973).

The oxygen isotope record has been used to create a proxy for global eustatic sea level fluctuation. During cold glacial periods, large volumes of water are stored on land in the form of ice, and global sea levels are lower. During warm interglacial periods, this water returns to the ocean and sea levels are high.

The oxygen isotope fluctuations have been compared with well dated marine terrace sequences to develop a standard eustatic sea level curve for the Pleistocene. There are at least three terrace sequences that are well dated using uranium-series methods: Barbados (Mesolella et al., 1969; Bender et al., 1979), Haiti (Dodge et al., 1983) and New Guinea (Bloom et al., 1974; Aharon, 1983). The Huon Peninsula, New Guinea terrace sequence has become recognized as a standard for age correlation of marine terraces world wide (Bull, 1985; Lajoie, 1986).

The life of a marine terrace begins as a wavecut tidal platform. During tectonic uplift, the wavecut surface is elevated above sea level, creating the tread of the terrace. When sea level is high, waves erode at the front of the uplifted terrace, creating a sea cliff, referred to as the terrace riser (Fig. 8). The fluctuation of eustatic sea level in combination with ongoing tectonic uplift creates a stepping series of terraces oriented parallel to the coast.

Marine terraces preserve paleo-shorelines that mark sea level during the creation of the terrace tread. The paleo-shoreline elevation is defined by a line where the tread meets the riser, known as the inner edge. In order to recreate the location and elevation of the inner edge, both tectonic uplift and sea level fluctuation need to be considered. Inner edge elevations may be difficult to identify due to the abundance of sediment blanketing the bedrock tread. In these cases, it can be estimated based on sediment thickness.

Aerial Photographs

Aerial photos provide an alternative perspective on landforms normally viewed from the ground. This type of remote sensing began in the early 1900's when Wilbur Wright took a photograph from his plane while flying over Italy (Way, 1973). Since then, aerial photographs have become less of a novelty and more of a science. During World War II, improved aerial photos were used in mapping and in the reconnaissance work of mining and oil companies. Cameras used for the purpose of aerial photography have improved greatly since the early 1900's. High quality cameras and lenses are now manufactured solely for the purpose of aerial photography.

Aerial photographs are taken with the plane of the film oriented parallel to the ground. A series of photos are taken in flight with 60% overlap in each frame. The geometry of this task is based on altitude, focal length of the lens, and orientation of the camera. This geometry allows for the scale of the photo be determined, although there is some distortion. For example, hills closer to the camera will seem higher than the valley bottoms look lower. Also, the center of the photo is more accurate then the edge of the photo since it is closer to the camera lens (Way, 1973).

There are four different film types: black and white, infrared, color, and color infrared. The final critical step in the production of aerial photos is their development. Paper weight, contrast, print finish, paper stability, and color balance all affect the outcome of the photo. Black and white photos are beneficial due to the versatility and cheaper processing costs. The disadvantage of using black and white photos is that the gray tones make features harder to distinguish when compared to color photos.

Once the photos of an area are developed they can be cut and pasted together for an overall mosaic view of the area. Photos can also be viewed in pairs with a stereoscope, allowing the area to be viewed in three dimensions. A stereoscope will exaggerate elevations, but this enables landscapes features to be seen more easily.

Global Positioning System (GPS) Surveying

A total of 24 satellites make up the radio-navigation global positioning system (Trimble, 2002). GPS surveying uses triangulation to find a location and elevation at a

certain point on earth's surface. Every square meter on the earth's surface has a unique address which can be identified with coordinates given by a GPS receiver. Multiple satellites send signals which are recorded by the receiver. The timing of the signals is used to find the location of the receiver.

Differential GPS surveying is more accurate and can account for error occurring between the satellites and the receiver. This technique can be used to measure mobile positions to within several meters accuracy and to within a meter for stationary objects. Differential surveying requires a signal from a reference station with a known, fixed location. Instead of using timing signals from satellites to calculate a position, the reference station uses its known position to calculate timing relative to the GPS receiver. Travel time of the GPS signals are calculated, and then compared to actual travel time. The difference is known as the error correction factor. This information is transmitted by the reference receiver to the roving receiver so that the data can be corrected.

Terrace Mapping and Fieldwork

The nature and extent of the Waratah Bay terrace sequence were determined through initial field reconnaissance and examination of aerial photographs. Field mapping and GPS surveying was then conducted along a series of transects across the terraces and the positions of terrace treads, risers, outer, and inner edges were recorded. The spatial coordinates of these features (location and elevation) were surveyed along each transect using a Trimble XRS-Pro GPS receiver and TSC1 data logger with real time differential correction yielding vertical accuracies of <1 meter (see Appendix A for data). The GPS elevation data from each transect were plotted onto an aerial photo of the Waratah Bay area (#3965-247, 1:26,000 scale). Transects are labeled WB 1 to WB 10 from west to east (Fig. 9).

Three representative transects (WB 1, 7, and 10) were projected onto profile lines oriented perpendicular to the northeast trend of Cape Liptrap (Fig. 10). Elevation data from these transects were projected onto lines of azimuth 325° using the formula $[\cos(\theta)(northing)] + [\sin(\theta)(easting)]$, where θ is the projection azimuth and *northing* and *easting* are GPS coordinates (Appendix A). Guided by these elevation data and the stereoscopic analysis of aerial photos, the terrace treads were then mapped onto the air

photo base (Fig. 11). Topographic profiles of the terrace sequence were then plotted along these three projection lines (Fig. 12).

Terrace Deposits and Inner Edges

Terrace deposits were examined and described in the field at several locations. A detailed stratigraphic column was created describing a section of the terrace deposit of Terrace V (Fig. 13). These observations provided a guide for estimating the thickness of terrace deposits throughout the study area. A 10 meters (± 5 m) deposit thickness was estimated for most other terraces based on data from marine terraces located to the southwest at Walkerville and on Cape Liptrap (Figs. 14 & 15; Pezzia, 2003; Tunnell, 2003). Due to the overall lack of bedrock tread exposures in the field area, terrace inner edges were estimated using back edge elevations from the GPS profiles while assuming a 10 meters (± 5 m) thick terrace deposit.

Inner edge elevations along each transect were plotted along a SW-NE trending line perpendicular to the projected transects (Fig. 16). This plot reveals elevation changes across the field area which may indicate deformation of terrace surfaces (tilt or offset).

Sea Level Correlation and Uplift Rates. Terrace ages and uplift rates (Table 1) were estimated by correlation with Late Cenozoic sea level high stands (Fig. 17; Bull, 1985; Lajoie, 1986). Inner edge elevations were plotted in conjunction with paleo-sea level curves for the Late Tertiary and Quaternary (Chappell and Shackleton, 1986; Darter, 2000). Assuming a constant uplift rate, terrace inner edges were linked to sea level high stands using a straight line where *slope = uplift rate*. Multiple scenarios were examined in order to determine a best-fit correlation (see Appendix B).

Results

Marine Terraces

Seven relatively continuous marine terraces (I-VII) were identified in the study area (Fig. 11). Topographic profiles show tread elevations ranging from near sea level for terrace VII to >140 meters for terrace I (Fig. 12). While terraces I-V occur as typical

wave cut surfaces mantled by terrace deposits, terrace VI consists of a series of lobate depositional fans centered around the mouths of streams incised into the upper terraces.

The coastline of the study area curves toward the east from the northeast trend of high topography along Cape Liptrap to an east-west trend along low-relief topography of Waratah Bay (Fig. 11). Risers to the lower terraces (V-VI) are sub-parallel to the modern shoreline, whereas those of the upper terraces (I-IV) extend inland along the linear northeast trend of the Cape Liptrap Peninsula. The width of terrace V, therefore, increases significantly toward the east and its tread corresponds with the lowland surface of the Yanakie isthmus east of the study area (Fig. 2).

Terrace Deposits

Overall, terrace deposits in the field area consist of well sorted, fine-grained silicic beach and dune sands interbedded locally with silts and clays (Fig. 13). Based on observations in both this and adjacent study areas, deposit thicknesses range from approximately 5 to 15 m. Terraces I-IV are mantled with dune deposits that occur in distinct linear ridges.

Soils formed on terrace V approach 5 meters in thickness and resemble spodosols, with a distinct light gray leached horizon. A stratigraphic column (Fig. 13) was described for the terrace deposit on terrace V at location C (Fig. 9 for location). Here, 1.2 m of soil capped a total deposit thickness of greater than 32 meters. Bedrock was not located directly but was assumed to be underlying a clay rich bed of angular quartz gravels at the base of the section. Similar gravel deposits known as Haunted Hill Gravel, occur throughout the region across bedrock surfaces and are the product of the stripping of pre-weathered granite terrain at Wilson's Promontory. These quartz gravels of Wilson's Promontory, along with an abundance of kaolin, was deposited to the north and northwest of Wilson's Promontory through the Mid Cretaceous (Ollier and Pain,1994)

Terrace Deformation

The projected terrace profiles (WB 1, 7, and 10) show a significant decrease in tread elevation toward the east indicating a systematic tilt away from Cape Liptrap (Fig. 16). In addition, terrace V shows an anomalously high elevation along transect WB 1

when compared with WB 7 and WB 10, indicating localized deformation in the southwest portion of the field area. The estimated elevation of the bedrock strath at location C was approximately 30 meters above mean sea level. This bedrock elevation was compared with bedrock tread outcrops to the immediate west at location D (Fig. 9 for location). The bedrock was exposed at approximately 54 meters above mean sea level. The distance between locations C and D is within 0.5 km. In this short distance, there is an obvious tread elevation change of about 24 meters.

Sea Level Curve Correlation and Uplift Rates

A best fit correlation between terraces and the paleo-sea level curve (Fig. 17) resulted in estimated ages ranging from 80 ka (terrace VI) to 490 ka (terrace I). This age range is consistent with that estimated for terraces along the Gippsland coast east of Corner Inlet (Ward et al.,1971; Ward 1985). In this scenario, the lowest and most prominent terraces (V-VI) are correlated with the oxygen isotope stages 5-7 high stands, and higher terraces to stages 9-13. Based on these estimated ages, uplift rates range between 0.1 and 0.4 m/ka within the study area (Table 1). Alternate correlations which proved unlikely are included in Appendix B.

Dune Deposits

Samples from dune deposits overlying terraces in adjacent study areas (Fig. 14) were dated using Optically Stimulated Luminescence (OSL) (Pezzia, 2003; Tunnel, 2003). This technique calculates the age of a sample since it was last buried. Ionizing radiation of uranium, thorium, and potassium is stored in the sediment and emits luminescence which can be detected by laboratory analysis. The age of the sediment is found with the following formula: Age = *total accumulated radiation dose/ annual radiation dose* (SCIDR, 2003). The dated quartz sand dunes averaged 21 ka in age, linking them to an aeolian phase during the last glacial maximum (Gardner et al., 2003). These sands have a possible provenance of Wilson's Promontory or Paleozoic Basement

rock (Pezzia, 2003). These dunes are significantly younger than the terrace surfaces beneath them.

Discussion and Conclusions

The well-developed flight of marine terraces at Waratah Bay provides evidence for Late Cenozoic uplift along the Cape Liptrap peninsula. The northeastward tilt of terrace treads indicates maximum uplift centered along the Cape Liptrap axis and a decrease in uplift rate toward the Yanakie lowlands along Corner Inlet.

The tread of terrace VI, when projected eastward to the Yanakie isthmus, can be correlated with a 1.7 meter elevation terrace at Corner Inlet dated at 122 ± 13 ka (T. Gardner, pers. com., 2003). A nearly identical OSL age of 122 ± 9 ka was also obtained for a 3.3 meter terrace at Morgan's Beach (Fig. 2; Gardner et al., 2003). These ages suggest that terrace VI formed during the maximum Late Pleistocene sea level highstand (OIS 5e). These ages are consistent with ages estimated in this study from sea level curve correlations. Based on these correlations, the seven terraces mapped in this study at Waratah Bay range in age from 80 ka to 490 ka.

While all terrace treads in the study area show a systematic tilt toward the northeast (Fig.16), terrace V exhibits an unusual break in slope between profiles WB 1 and 7. This location coincides with the mapped trace of the Walkerville fault (Fig.11). Where the fault extends onshore, a bedrock intertidal platform and a narrow 1-2 meter elevation wave cut bench occur northwest of the fault trace. The location of these features coincides with the high topographic relief of Cape Liptrap, consistent with greater uplift northwest of the fault. The topographic profile WB 1 crosses the fault in the southwest corner of the field area (Fig. 11). Deformation has caused the upper five terraces to be uplifted together leaving a rather large elevation gap between terraces V and VI (Fig. 16). Profile WB 7 also crosses the fault above terrace V rather than below terrace V. The elevation gap moves from in between terraces V and VI to between terraces IV and V. There is no obvious deformation seen in profile WB 10. Based on terrace inner edge elevations and estimated ages (Table 1), uplift rates at Waratah Bay range from 0.2 to 0.4

m/ka northwest of the Walkerville fault, and from 0.1 to 0.2 m/ka southeast of the fault. These uplift rates are significantly higher than those determined for the terraces at Walkerville (0.08 – 0.1 m/ka; Pezzia, 2003) and at Cape Liptrap (0.013 – 0.021 m/ka; Tunnell, 2003). This reflects differences in terrace ages by various authors using alternative sea level correlations.

In general, the marine terraces at Waratah Bay may be the product of uplift and tilting resulting from Late Cenozoic slip on the northeast-trending Walkerville fault. Active crustal deformation along this segment of the southeastern Australian passive margin may result from denudation and isostatic flexure, variations in the crust/mantle thermal structure, and/or far-field intraplate stress.

The results of this study confirm that the "classic passive continental margin" of Australia is anything but passive. This investigation of marine terraces between Cape Liptrap and Wilson's Promontory has important implications for future models of the tectonic evolution of the southeastern Australian continental margin.

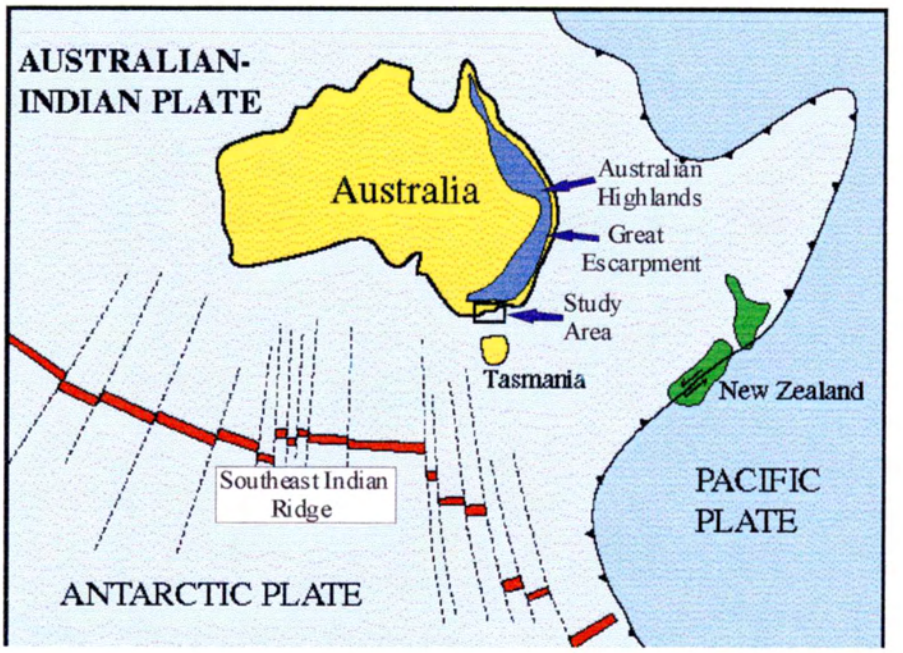

Figure 1: Plate tectonic map of Australia. Box indicated area of Fig. 2. (After Gardner, 2003)

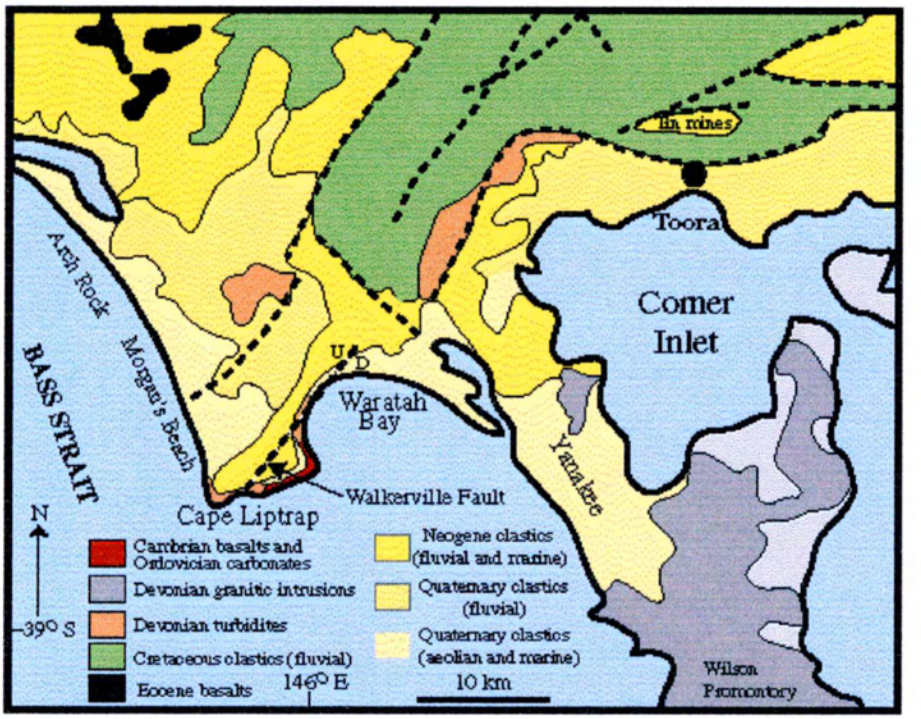

Figure 2: Generalized geologic map of Cape Liptrap and Wilson's Promontory, Victoria (After Gardner, 2003)

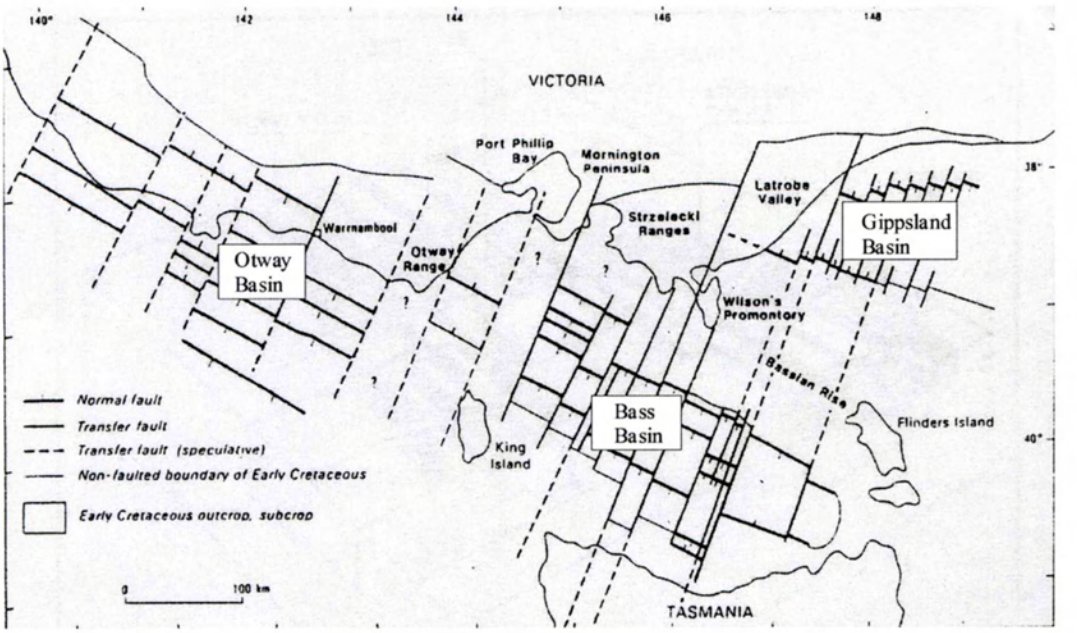

Figure 3: Bassian Zone Structure, southeast Australia
(After Abele, 1988)

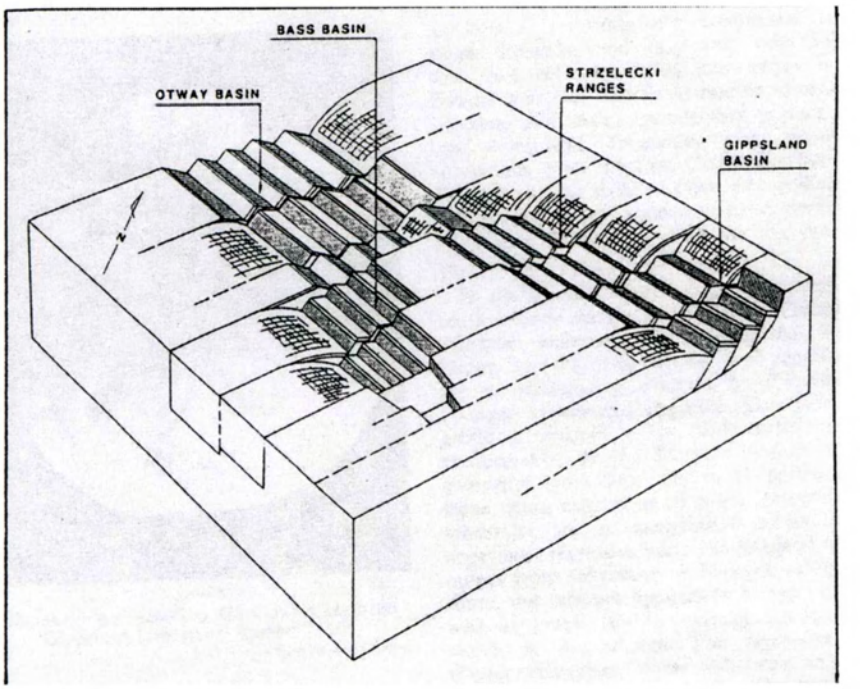

Figure 4: Schematic diagram of Cretaceous Rifting
within the Bassian Zone..
(After Abele, 1988)

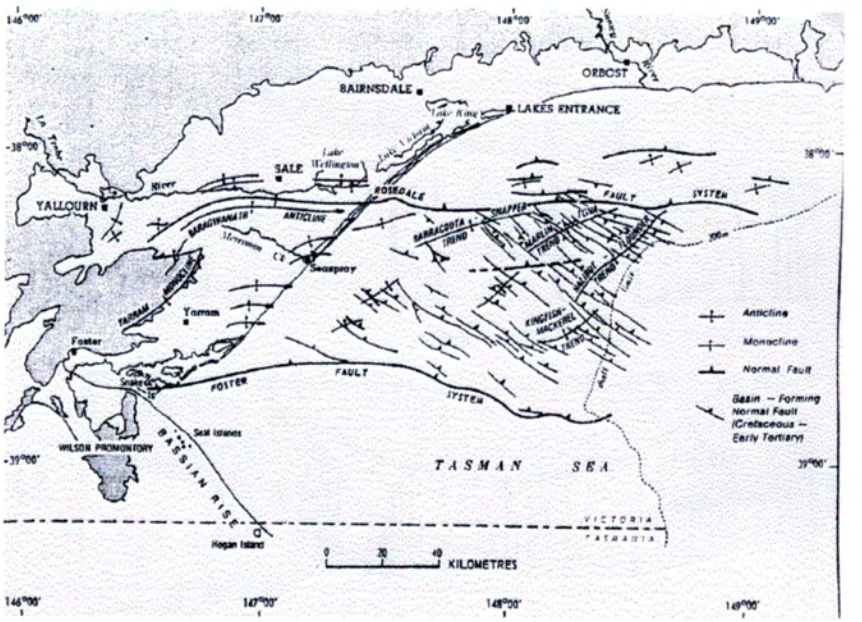

Figure 5: Gippsland Basin Structure
(After Abele, 1988)

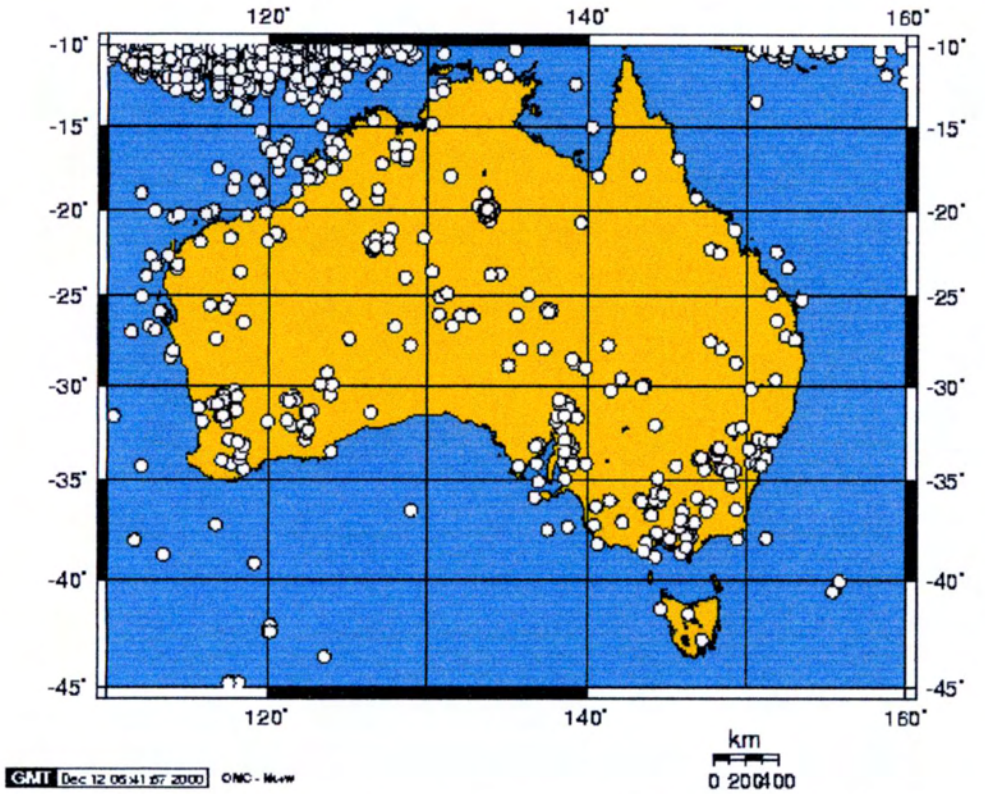

Figure 6: Seismicity of Australia from January 1970 to December 2000.
Circles represent earthquakes with a magnitude of 4.5 or greater
(US Geological Survey).

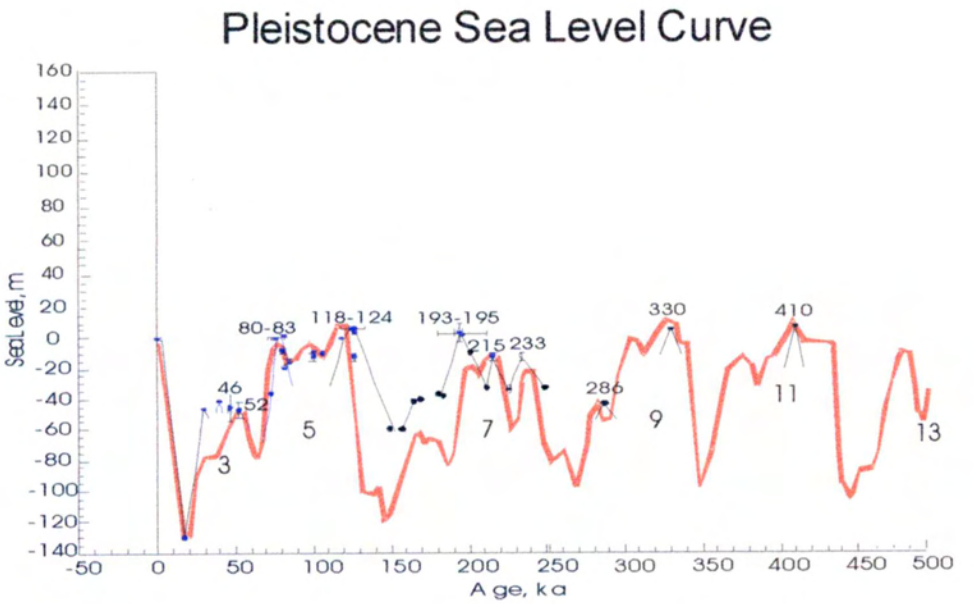

Figure 7: Red sea level curve based on marine oxygen isotope records (Imbrie et al., 1984; Chappell and Shakleton, 1986). Black dots indicate measured sea level data compiled by various sources by Darter (2000).

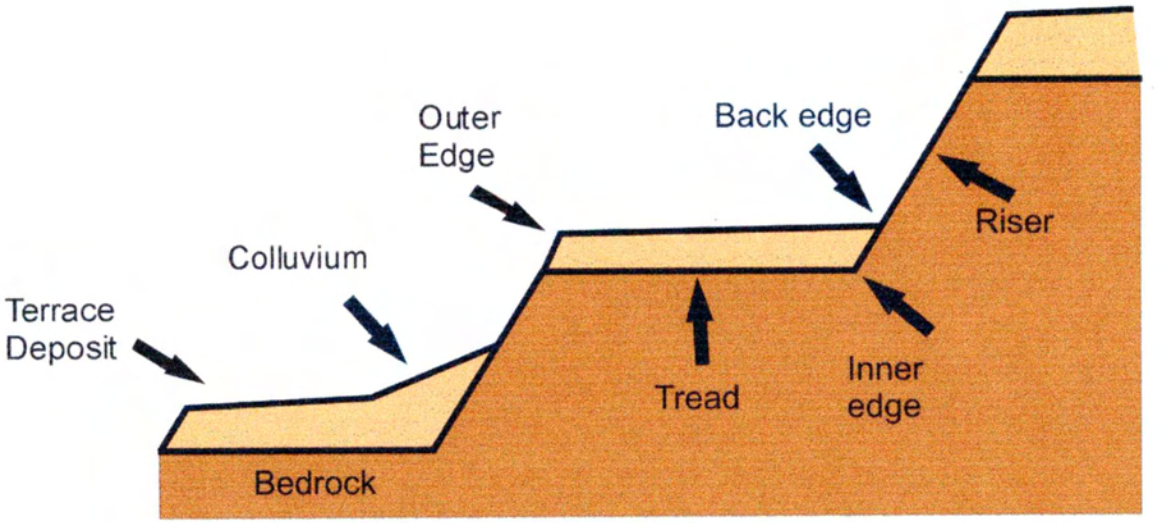

Figure 8: Marine terrace features.

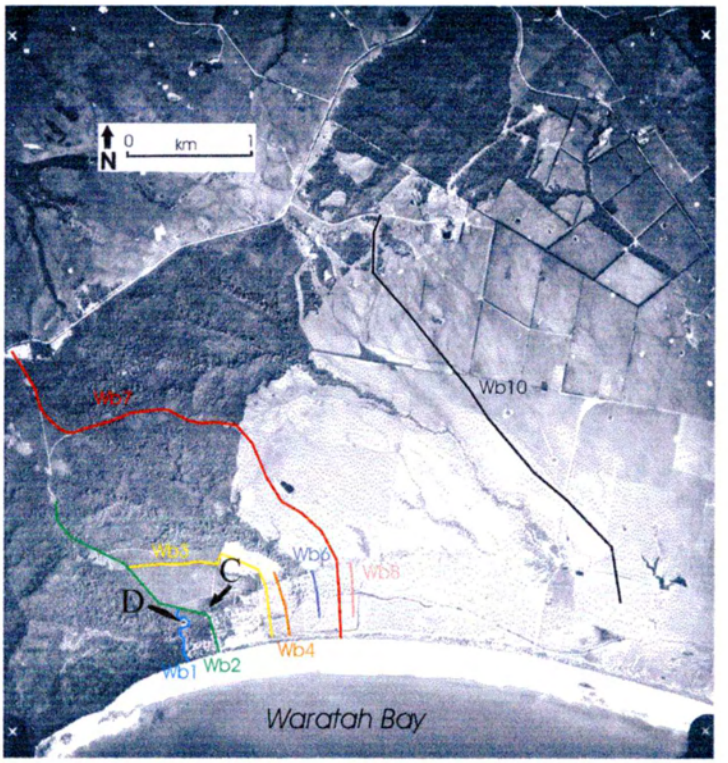

Figure 9: Paths of transcect WB 1-10 on aerial photo base. Locations of Sites C and D noted.

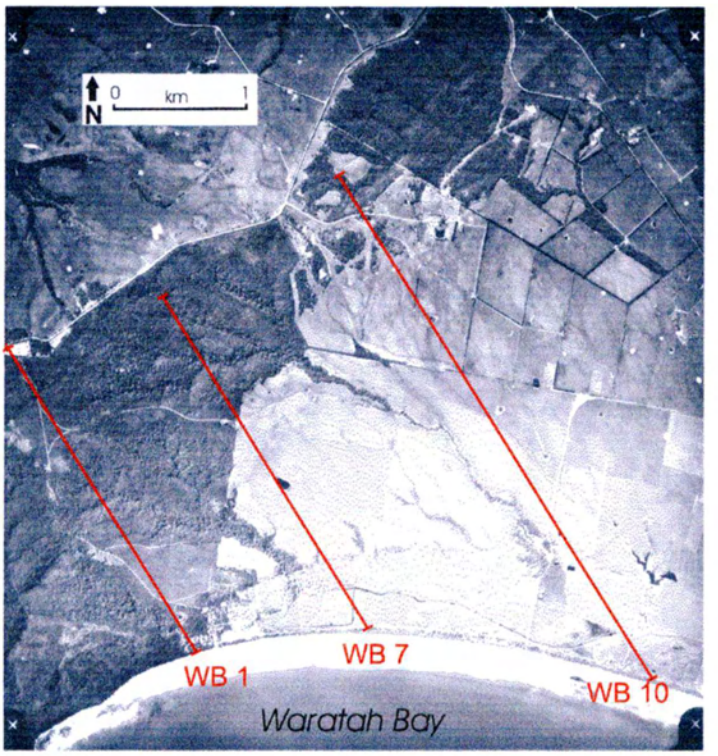

Figure 10: Projected profiles WB 1, 7, and 10.

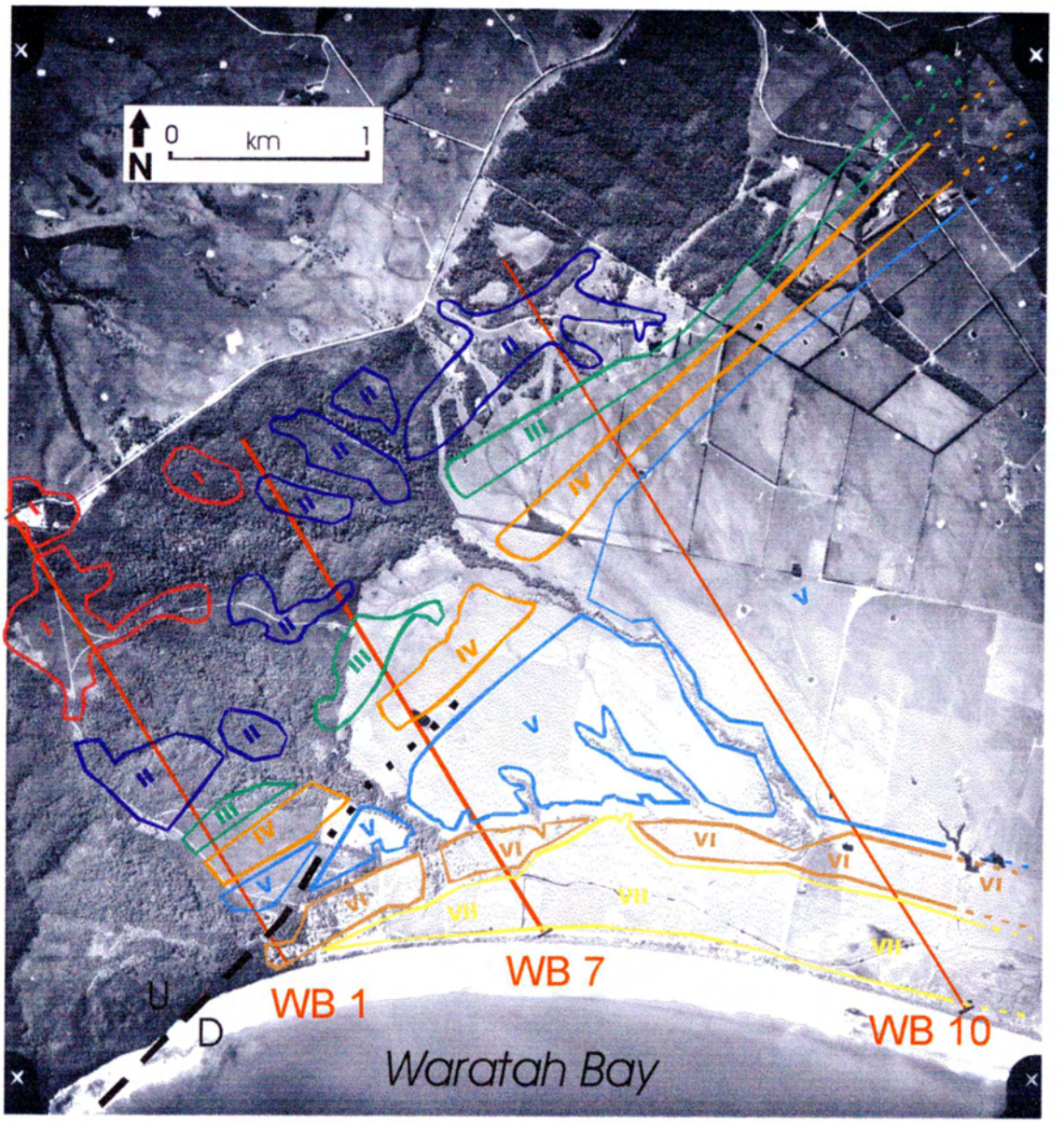

Figure 11: Marine terrace treads of Waratah Bay mapped on an aerial photo base. Red lines indicate marked locations of projected terrace profiles WB 1, 7, and 10.

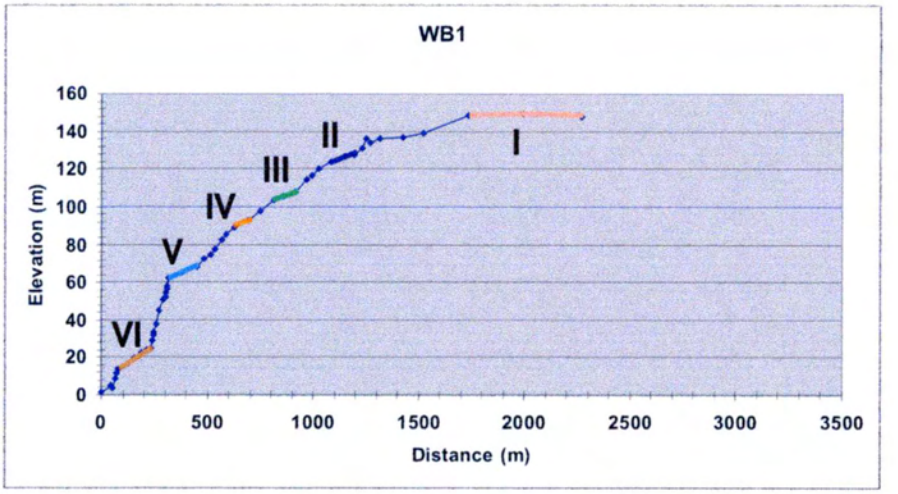

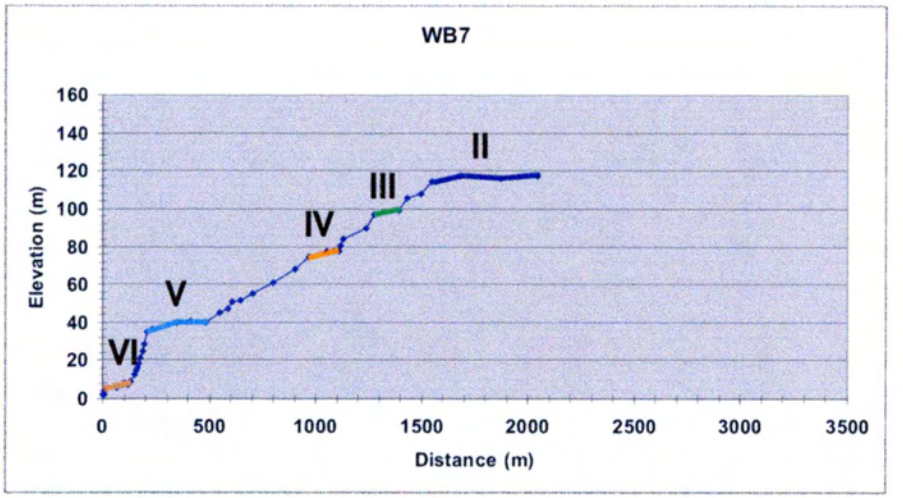

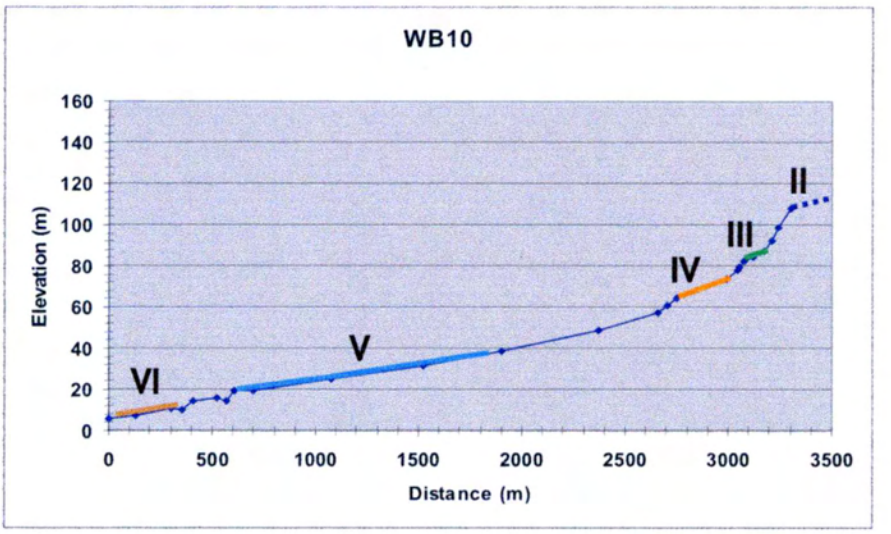

Figure 12: Projected terrace profiles WB 1, 7, and 10. See fig. 11 for location.

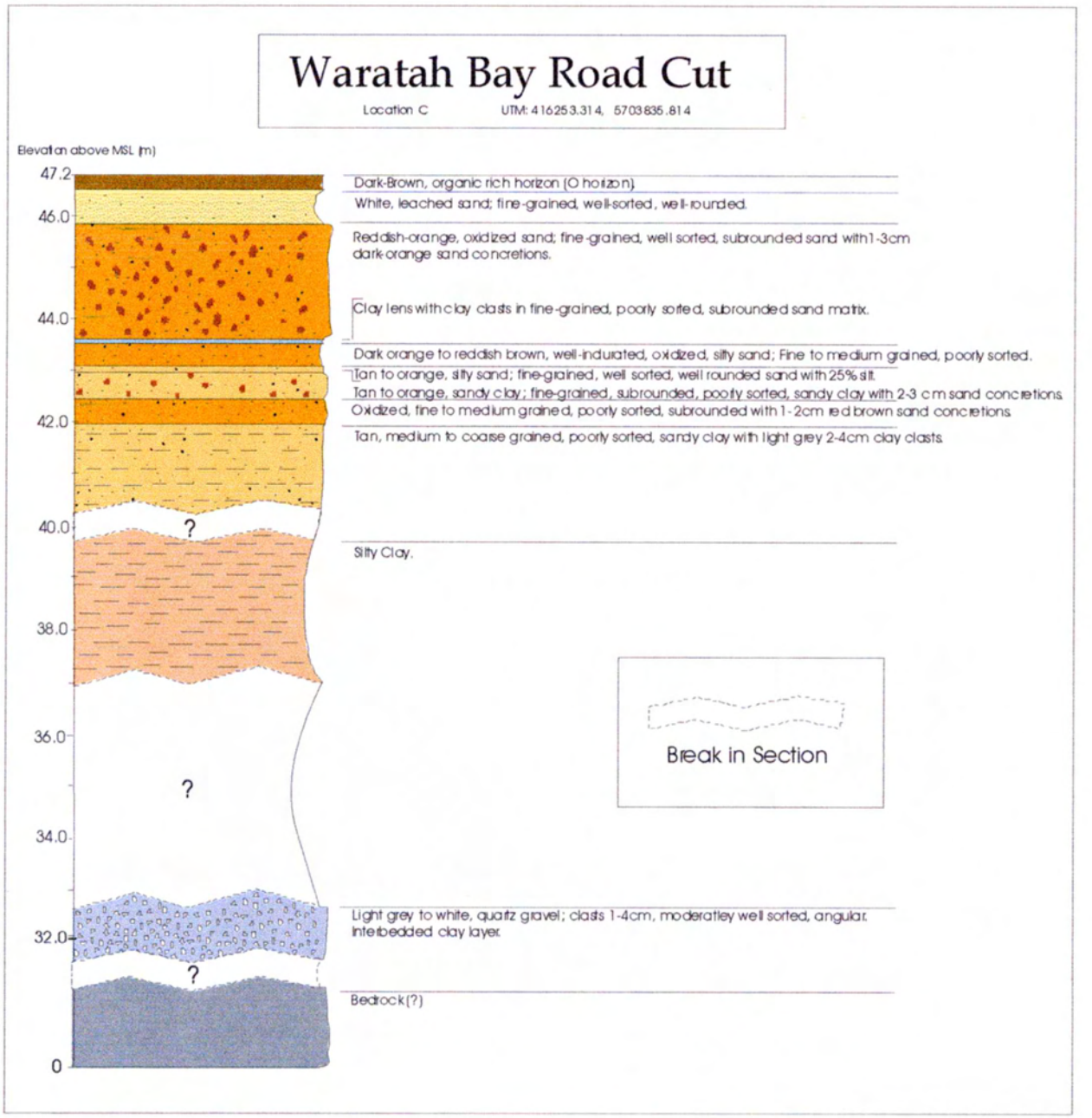

Figure 13: Stratigraphic column describing Terrace V deposit at location C (see Fig. 9 for location).

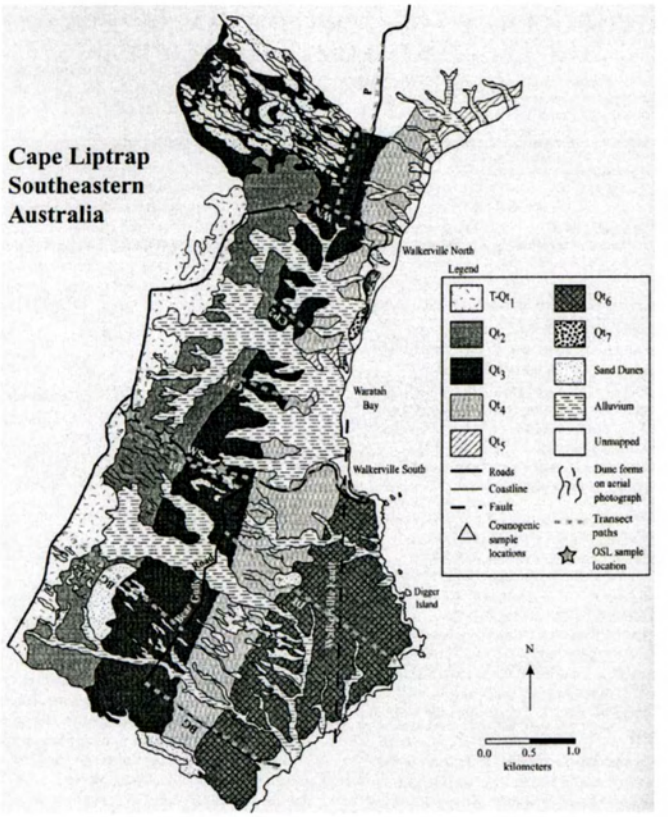

Figure 14 (left): Mapped treads of marine terrace treads near Walkerville, Cape Liptrap, southeast Australia (After Pezzia, 2003).

Figure 15 (below): Mapped marine terrace treads of southern Cape Liptrap (After Tunnell, 2003)

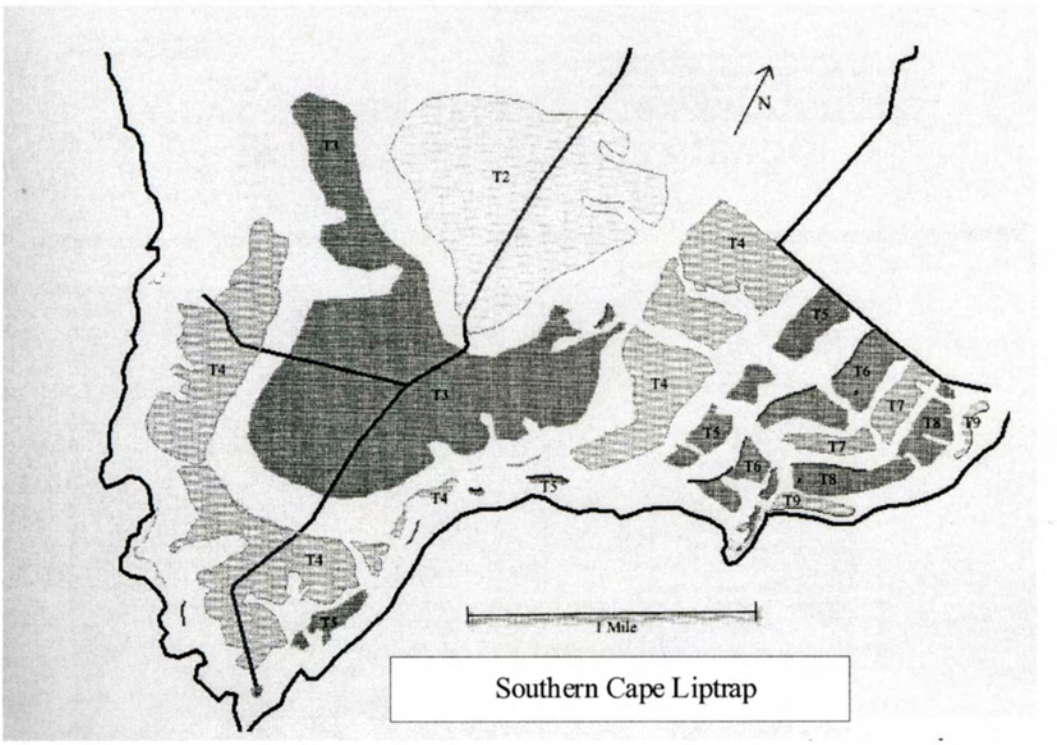

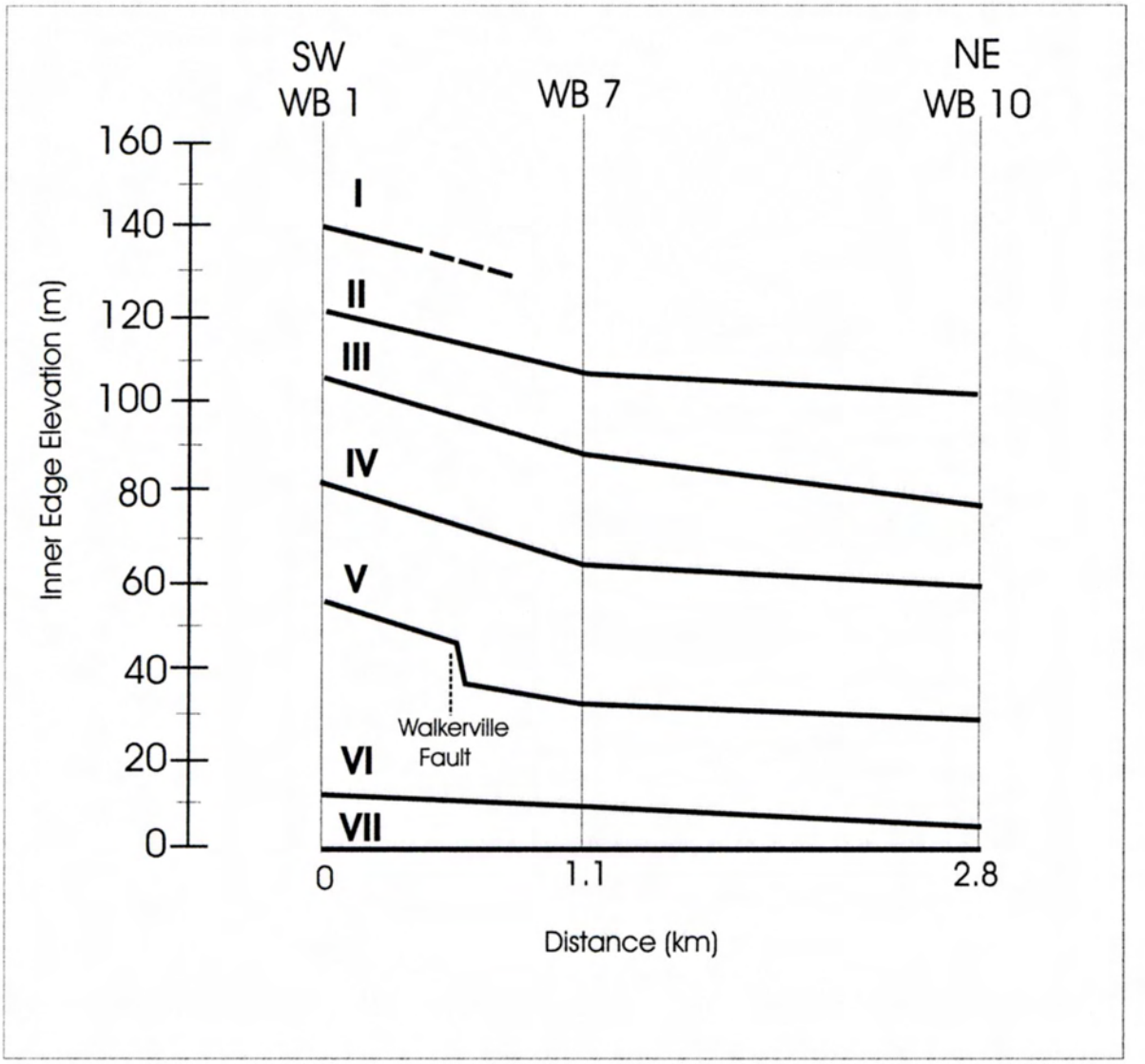

Figure 16: Terrace inner edge elevations plotted in a line perpendicular to the profiles WB 1, 7, and 10.

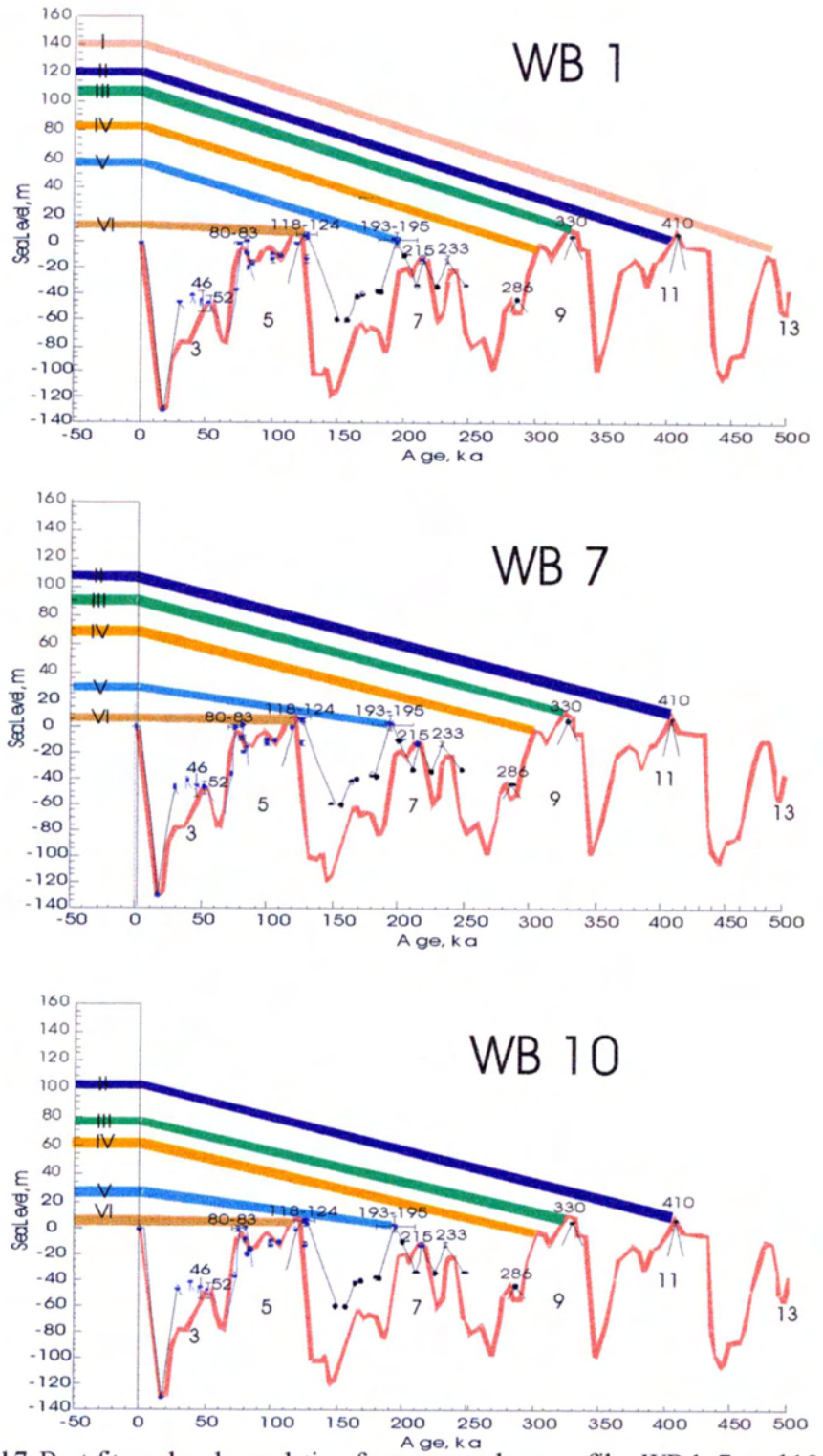

Figure 17: Best fit sea level correlation for terraces along profiles WB 1, 7, and 10. Terrace inner edge elevations (at left) are linked to sea level highstands with heavy lines that represent uplift pathways (slope = uplift rate). Red sea level curve based on marine oxygen isotope records (Imbrie et al.,1984; Chappell and Shakleton, 1986). Black dots indicate measured sea level data compiled by various sources by Darter (2000). See appendix B for alternate correlations.

Terrace	Inner Edge Elv. (+ 5 m)	Estimated Age (ka)	Uplift rate (m/ka)
Profile WB 1			
I	140	480-490	0.28-0.30
II	121	405-415	0.28-0.31
III	108	320-330	0.31-0.35
IV	82	300-310	0.25-0.29
V	58	193-195	0.27-0.33
VI	13	118-125	0.06-0.14
Profile WB 7			
II	108	405-415	0.25-0.28
III	90	320-330	0.26-0.30
IV	69	300-310	0.21-0.25
V	30	193-195	0.13-0.18
VI	8	118-125	0.02-0.11
Profile WB 10			
II	102	405-415	0.23-0.26
III	78	320-330	0.22-0.26
IV	62	300-310	0.18-0.22
V	28	193-195	0.12-0.17
VI	4	118-125	0.0-0.08

Table 1: Estimated ages and uplift rates of terraces along WB 1, 7, and 10.

Acknowledgements

I would like to thank the Keck Geology Consortium for my opportunity to participate in the 2002 Australia research project, Tom Gardner, Dorothy Merritts, and John Webb for their direction and knowledge in the field, land owners in Waratah Bay for allowing me on their property, The Toora Tourist Park and Toora Royal Standard Hotel for taking care of the students during the project, and Sarah Flanagan, Dan Kapostasy, Claudia Pezzia, Kathy Bremar, and Rob Tunnell for their aid in the field. I would also like to thank the Cal Poly Geology Department for supporting my travel to GSA Cordilleran section meeting to present my project poster, my parents John and Mary Amborn for their continuous and much needed support, and last but not least, my advisor and sponsor Dr. Jeff Marshall, for his patience, guidance, support, and time. Thank you.

References

Abele, C., 1988, Tertiary, ch. 8, *in* Douglas, J. and Ferguson, J., eds., Geology of Victoria: Geological Society of Australia, Melbourne, p. 251-350.

Aharon, P., 1983, 140,000-yr isotope climatic record from raised coral reefs in New Guinea *in* Nature, v. 304, p. 720.

Amborn, T.A., 2003, Evidence for active tectonics along the Australian passive margin: Quaternary marine of Waratah Bay, Victoria: Sixteenth Keck Research Symposium in Geology Proceedings, p. 10-13.

Amborn, T.A., Marshall, J.S., and Gardner, T.W., 2003, Evidence for active tectonics along the Australian passive margin: Quaternary marine terraces of Waratah Bay, Victoria: Geological Society of America, Abstracts with Programs, v.35, no.4, p. 16.

Anderson, R.S., Densmore, A.L., and Ellis, M.A., 1999, The generation and degradation of marine terraces: Basin Research, v. 11, p. 7-19.

Bender, M.L., Fairbanks, R.G., Taylor, F.W., Matthews, R.K., Goddard, J.G., and Broecker, W.S., 1979,Uranium series dating of the Pleistocene reef tracts of Barbados, West Indies *in* Geological Society of America Bulletin, v. 90, p. 577-594.

Bloom, A.L., Broecker, W.S., Chappell, M.A., Matthews, R.K., and Mesolella, K.J., 1974, Quaternary sea level fluctuations on a tectonic coast: New $^{230}Th/^{234}U$ dates from the Huon Peninsula, New Guinea, *in* Quat. Res., v.4, p. 185-205.

Bloom, A.L., Yonekura, N., 1990, Graphic analysis of dislocated quaternary shoreline *in* Studies in Geophysics: Sea Level Change, p. 104-106.

Bolger, P.F., 1991, Lithofacies variation as a consequence of Late Cainozoic tectonic paleoclimatic events in the onshore Gippsland Basin: in, Williams, M.A.J., DeDecker,P., and Kershaw, A.P., The Cainozoic in Australia: a re-appraisal of the evidence, Geological Society of Australia, spec. pub. #18, p.158-180.

Bremar, K., 2003, Reconstructing the Paleoenvironment and source of the Haunted Hill Formation (Pliocene-Pleistocene), South Gippsland, Victoria, Australia: Sixteenth Keck Research Symposium in Geology Proceedings, p. 14-16.

Bull, W.B., 1985, Correlation of flights of global marine terraces, *in* Morisawa, M., and Hack, J.T., eds., Tectonic Geomorphology: Proceedings of the 15th Geomorphology Symposia Series, Binghamton, p. 129-154.

Chappell, J., and Shackleton, N.J., 1986, Oxygen isotopes and sea level: Nature, v. 324, p. 137-

Darter, J., 2000, Compilation of a late-Quaternary sea level curve: Thirteenth Keck Research Symposium in Geology Proceedings, p. 140-143.

Dodge, R.E., Fairbanks, R.G., and Maurrasse, F., 1983, Pleistocene sea levels from raised coral reefs of Haiti, *in* Science, v. 219, p. 1423-1425.

Gardner, T., 2003, Late Neogene and Quaternary tectonics and landscape evolution along the southeastern Australian passive margin, Cape Liptrap, Australia: Sixteenth Keck Research Symposium in Geology Proceedings, p. 5-7.

Gardner T., Merritts, D., Davis, A., Cassel, E., Pezzia, C., Webb, J., and Smith, B. 2003, Late Pleistocene, calcareous and siliceous aeolian and alluvial fan deposits, Cape Liptrap, Southeastern Victoria, Australia: Geological Society of America abstracts with programs, V. 34, abstract no. 134-27.

Gibson, G., Wesson, V., and Cuthbertson, R., 1981, Seismicity of Victoria to 1980, Journal of the Geological Society of Australia, p. 341-353.

Hocking, J.B., Gloe, C.S., Threfall, W.F., Holdgate, G.R., and Bolger, P.F., 1988, Gippsland Basin, *in* Douglas, J.G., and Ferguson, J.A., eds., The geology of Victoria: Melbourne, Geological Society of Australia Incorporated, Victoria Division, p. 322-347.

Imbrie, et al., 1984, The orbital theory of Pleistocene climate: Support from a revised chronology of the marine d^{18}O record, *in* Berger, A., ed., Milankovitch and Climate, Dordrect, Netherlands, D. Reidel, p. 269-305.

Jenkin, J., 1968, The geomorphology and upper Cainozoic geology of southeast Gippsland, Victoria *in* Geological Survey of Victoria, p. 15-21, 127-136.

Jenkin, J.,1988, Quaternary, ch. 9 and 10, *in* Douglas, J. and Ferguson, J., eds., Geology of Victoria: Geological Society of Australia, Melbourne, p. 351-426.

Lajoie, K., 1986, Coastal tectonics, *in* Wallace, R., ed., Active Tectonics, Washington, D.C., National Academy Press, p. 95-124.

Matthews, R., 1990, Quaternary sea level change *in* Studies of Geophysics: Sea Level Change, p. 93.

Mesolella, K. J., Matthews, R. K., Broecker, W. S., and Thurber, D. L., 1969, The astronomical theory of climatic change: Barbados data *in* J. of Geology, v. 77, p. 250-274.

Mosley, J.G., 2002, International and world heritage values of Wilson's Promontory national park: Peak Environmental Enterprises, p. 6-8.

Ollier, C., and Pain, C., 1994, Landscape evolution and tectonics in southeastern Australia: J. Australian Geology and Geophysics, v. 15, p. 335-345.

Orr, M, 1998, Tectonic Geomorphology of the Bagong and Dargo High Plains region, east Victorian Highlands, Australia, PhD Dissertation, University of Melbourne, Australia.

Pezzia, C., 2003, Late Neogene to Quaternary Marin Terraces and Aeolian Deposits, Cape Liptrap, Southeastern Australia: Sixteenth Keck Research Symposium in Geology Proceedings, p. 37-40.

Ritter, D., Kochel, R., and Miller, J., 1995, Process Geomorphology, McGraw Hill.

Sandiford, M., 2002, Late Neogene faulting record in Southeastern Australia: Victoria undercover, Benalla 2002 Conference Proceedings and Field Guide, p. 131-135.

Shackleton, N.J., and Opdyke, N. D., 1973, Oxygen isotope and paleomagnetic stratigraphy of equational Pacific core: oxygen isotope temperatures and ice volumes on a 10^5 and 10^6 year scale, *in* Quaternary Research 3, p. 39-55.

SCIDR, 2003, Sheffield Centre for International Drylands Research: Luminescence Dating. www.shef.ac.uk.

Trimble GPS Surveying, 2002, www.trimble.com.

Tuddenham, W.G., 1970, The coastal geomorphology of Wilson's Promontory, Victoria: Quaternary Sedimentation around the shores of the Bass Strait, University of Sydney.

Tunnell, R., 2003, Marine Terrace Mapping, Formation and Uplift; Cape Liptrap, Southeastern Australia: Sixteenth Keck Research Symposiumin Geology Proceedings, p.41-44.

Ward, W.T., 1985, Correlation of east Australian Pleistocene shorelines with deep-sea core stages: A basis for coastal chronology *in* Geological Society of America Bulletin, v. 96, p. 1156-1166.

Ward, W.T., Ross, P.J., and Colquhoun, D.J., 1971, Interglacial high sea levels – an absolute chronology derived from shoreline elevations *in* Palaeogeography, Palaeoclimatology, Palaeoecology, v. 9, p. 77-99.

Way, D., 1973, Terrain analysis; a guide to site selection using aerial photographic interpretation; Dowden, Hutchinson, & Ross.

Appendix A: GPS Data

WB 1

Easting	Northing	Projection	Elevation	Description
416246.7	5703392	4731158.76	1.565	sea level
416221.5	5703428	4731202.855	4.454	berm base
416221	5703428	4731203.396	5.184	berm edge
416226.4	5703444	4731214.042	3.766	IE of back beach
416225.4	5703454	4731223.553	8.561	riser 0-1
416224.9	5703462	4731230.561	11.8	riser 0-1
416223	5703471	4731239.068	14.116	OE 1
416201.2	5703506	4731280.877	16.405	tread 1
416191.3	5703541	4731315.347	19.761	tread1
416172.6	5703568	4731348.908	22.246	tread 1
416181.3	5703605	4731376.606	23.601	tread 1
416182.8	5703627	4731394.589	24.707	IE 1
416190.4	5703642	4731403.299	29.017	riser 1-2
416191	5703652	4731411.836	31.914	riser 1-2
416191.1	5703656	4731415.408	33.078	riser1-2
416191.1	5703666	4731424.495	37.849	riser 1-2 I
416192.6	5703688	4731442.329	44.91	riser1-2
416188.4	5703706	4731459.98	50.808	riser 1-2
416187	5703717	4731469.952	52.101	OE 2
416180.1	5703716	4731472.544	52.3	OE 2-gully
416167.6	5703707	4731471.521	49.005	side of gully
416150.8	5703700	4731473.443	43.347	side of gully
416186.8	5703733	4731483.888	54.114	tread 2
416158.2	5703792	4731549.317	56.354	tread 2
416140.5	5703870	4731626.127	58.026	tread 2 trail insctn
416097.9	5703880	4731655.755	62.116	IE 2 trail insctn
416063	5703890	4731681.996	65.301	riser 2-3
416033.8	5703899	4731704.391	68.1	riser 2-3
416001.2	5703913	4731733.245	72.548	riser 2-3
415987.6	5703923	4731748.32	74.303	OE 3
415958.8	5703957	4731792.046	77.777	tread 3
415917.7	5704003	4731852.463	82.472	tread 3
415884.4	5704049	4731909.268	85.589	tread 3
415841.7	5704101	4731975.417	89.099	tread 3
415809.8	5704135	4732020.718	92.538	riser 3-4
415773.1	5704181	4732078.744	98.074	riser 3-4
415739.6	5704216	4732126.526	103.204	riser 3-4
415713.5	5704234	4732155.061	105.805	OE 4
415682.9	5704249	4732182.838	107.739	tread 4-dune
415618.6	5704276	4732238.702	114.104	tread 4-dune
415559	5704312	4732299.225	116.448	IE 4
415525.6	5704340	4732340.135	120.008	riser 4-5
415495.3	5704366	4732378.26	123.855	riser 4-5
415476.2	5704380	4732399.521	126.457	OE 5
415455.4	5704390	4732419.095	127.547	tread 5
415414.6	5704411	4732457.498	130.746	tread 5

415308.5	5704471	4732562.41	136.302	tread 5
415258.1	5704553	4732659.171	133.896	tread 5
415264.7	5704700	4732783.186	135.945	tread 5
415212	5704784	4732882.283	136.665	tread 5
415227.7	5704890	4732965.393	139.052	tread 5-stick

WB2

Easting	Northing	Projection	Elevation	Description
416141.6	5703871	4327502.116	61.421	tread 2
416179.2	5703859	4327520.413	57.784	OE 2
416210.6	5703844	4327532.035	53.719	riser 2-1
416252.2	5703838	4327557.152	45.931	riser 2-1
416300.1	5703825	4327581.705	38.166	riser 2-1
416335.3	5703812	4327597.974	31.245	riser 2-1
416358.5	5703757	4327575.444	23.11	IE 1
416375.5	5703747	4327580.249	20.766	tread 1-rd
416386.3	5703695	4327550.987	13.383	tread 1-rd
416392.8	5703667	4327535.99	11.045	tread 1-rd
416401.1	5703629	4327514.462	7.758	tread 1-rd
416407.2	5703595	4327494.865	7.53	tread 1-rd
416417.4	5703553	4327472.49	4.948	tread 1-rd
416434	5703529	4327467.3	4.639	OE 1
416436.6	5703511	4327456.397	5.649	dune crest
416444.7	5703493	4327449.314	3.268	high-high tide

WB 3

Easting	Northing	Projection	Elevation	Description
416876.6	5703570	5717570.877	1.676	high tide
416875.9	5703572	5717572.78	2.454	OE dune
416876.7	5703580	5717580.834	2.933	IE dune
416876.5	5703581	5717582.153	3.541	dune crest
416879.9	5703594	5717595.104	4.585	dune crest
416876.8	5703615	5717616.036	2.111	N end rd
416882.1	5703663	5717664.677	1.748	tread 0
416880.4	5703716	5717717.548	2.096	tread 0
416878.1	5703737	5717737.713	1.155	tread 0
416864.8	5703744	5717744.164	2.556	IE 0
416862.5	5703748	5717747.692	5.21	risert0/1
416861	5703753	5717752.908	6.643	OE 1
416902.5	5703759	5717760.711	7.594	OE 1
416895.6	5703802	5717803.368	6.524	tread 1
416876.4	5703889	5717889.149	8.491	tread 1
416849.6	5704028	5718026.73	12.817	tread 1
416848.1	5704038	5718036.682	16.834	riser 1-2
416844	5704050	5718048.881	19.459	riser 1-2
416840.4	5704061	5718059.175	23.752	riser 1-2
416835.5	5704079	5718076.861	30.825	riser 1-2
416832.7	5704093	5718090.937	35.004	riser 1-2
416824.1	5704114	5718111.64	37.018	tread 2
416827.3	5704115	-1944432.901	38.906	tread 2
416696.4	5704205	-1944331.208	43.085	tread 2
416621.5	5704220	-1944263.059	45.084	tread 2

416505.5	5704241	-1944157.249	48.694	tread 2
416441.3	5704251	-1944097.972	50.251	tread 2
416428.9	5704188	-1944069.132	50.847	tread 2
416359.8	5704176	-1943999.292	52.404	tread 2
416283.5	5704165	-1943922.832	58.595	IE 2
416207.4	5704152	-1943846.275	66.792	riser 2-3
416153.2	5704141	-1943790.899	70.527	riser 2-3
416087.6	5704134	-1943725.887	76.179	riser 2-3
416045.6	5704124	-1943682.782	78.959	OE 3
415981.9	5704112	-1943618.161	83.519	tread 3
415916.9	5704110	-1943555.017	86.901	tread 3
415845	5704100	-1943483.27	89.608	tread 3

WB 4

Easting	Northing	Projection	Elevation	Description
417022	5703563	5718204.697	0.434	Sea level
417020	5703587	5718228.942	2.018	high tide
417019.4	5703592	5718233.886	3.279	back beach
417019.1	5703595	5718236.423	3.112	IE beach
417020.4	5703598	5718239.424	5.47	OE dune
417020.6	5703611	5718252.774	5.528	dune crest
417019.2	5703623	5718264.145	3.753	Backdune rd
417093.2	5703636	5718284.175	3.179	Dw-rd intsctn
417091.7	5703661	5718308.656	2.578	Driveway pipe
417020.2	5703688	5718329.825	1.415	tread 0
417007.7	5703727	5718366.93	2.241	tread 0
416987.6	5703773	5718411.769	3.747	IE 0
416986	5703780	5718417.688	5.061	riser 0-1
416983.8	5703785	5718422.949	7.317	riser 0-1
416981.7	5703791	5718429.12	9.447	OE 1
416965.3	5703837	5718472.791	10.455	tread 1
416936.7	5703917	5718549.826	13.361	tread 1
416916	5703970	5718601.488	14.788	tread 1
416891.1	5704038	5718667.276	17.27	IE 1
416885.9	5704051	5718679.55	19.491	riser 1-2
416879.5	5704062	5718689.904	23.859	riser 1-2
416873.6	5704073	5718700.259	27.893	riser 1-2
416862.4	5704082	5718708.524	31.076	riser 1-2 house
416850.1	5704089	5718713.702	33.526	riser 1-2 to road
416838.7	5704094	5718717.844	36.392	OE 2
416829.4	5704112	5718735.527	38.148	tread 2

WB 5

Easting	Northing	Projection	Elevation	Description
416986.6	5704078	4328246.128	12.933	gully -tread 1
416996.3	5704049	4328232.993	10.902	gully tread 1
417007.5	5703988	4328197.462	10.349	gully tread 1
417045.1	5703928	4328181.721	8.536	gully
417043.1	5703890	4328153.43	8.162	gully tread 1
417053	5703854	4328134.613	7.616	gully at riser 0-1
417065.7	5703845	4328137.26	7.76	gully tread 0
417076.3	5703798	4328111.847	6.671	small fan tread 0

417078.3	5703784	4328102.926	5.865	small fan tread 0
417081.1	5703753	4328083.37	4.944	tread 0
417084.2	5703701	4328048.728	4.388	tread 0
417091.2	5703661	4328025.453	5.711	driveway pipe

WB 6

Easting	Northing	Projection	Elevation	Description
417091.3	5703661	4328025.445	5.292	Driveway pipe
417138.6	5703674	4328068.034	3.156	tread 0
417131.9	5703736	4328107.038	4.45	tread 0
417131.6	5703786	4328142.285	3.799	tread 0
417130.5	5703818	4328164.018	5.592	tread 0
417134.1	5703843	4328184.418	4.578	tread 0
417133.6	5703886	4328214.314	4.68	IE 0
417134	5703899	4328223.898	6.645	riser 0-1
417134.4	5703905	4328228.507	9.885	riser 0-1
417135.9	5703910	4328233.322	12.383	OE 1
417132.3	5703998	4328292.944	14.135	tread 1
417120.1	5704122	4328371.679	17.654	base riser 2

WB 7

Easting	Northing	Projection	Elevation	Description
417482.2	5703972	-2490435.915	1.869	tread 0
417478.5	5703983	-2490444.589	2.391	IE 0
417476.1	5703991	-2490450.62	5.238	OE 1
417459.2	5704053	-2490496.237	6.151	tread 1
417451.5	5704090	-2490521.136	6.943	tread 1
417449.8	5704108	-2490531.864	7.768	tread 1
417446.1	5704119	-2490540.524	7.449	tread 1
417441.8	5704143	-2490556.371	8.769	tread1-colluvium
417437.9	5704169	-2490572.874	12.14	tread 1 colluvium
417436.7	5704178	-2490578.123	14.248	tread 1-colluvium
417435.2	5704187	-2490584.21	16.072	tread 1 colluvium
417434.1	5704199	-2490591.052	18.305	IE 1
417433.4	5704209	-2490596.371	20.661	riser 1-2
417432.3	5704222	-2490603.896	24.439	riser 1-2
417432.4	5704238	-2490611.759	28.348	riser 1-2
417431.1	5704258	-2490622.859	34.393	OE 2
417417.8	5704288	-2490649.509	36.278	tread 2
417337.9	5704369	-2490759.146	39.732	tread 2-cement circle
417091.1	5703661	-2490618.976	4.291	Driveway pipe
417338.2	5704369	-2490758.887	39.178	start cement circle
417295.9	5704473	-2490847.576	40.851	tread 2
417189.8	5704438	-2490922.192	39.626	tread 2
417146.9	5704482	-2490981.119	43.51	tread 2
417117.9	5704509	-2491019.985	44.849	IE 2
417100.4	5704527	-2491044.09	47.114	riser 2 - 3
417070.6	5704551	-2491081.835	50.44	OE 3
417025.5	5704589	-2491139.669	51.4	tread 3
416950.2	5704644	-2491232.555	55.171	tread 3
416868.6	5704711	-2491336.631	60.919	riser
416814.1	5704749	-2491402.821	67.864	riser

416749.5	5704799	-2491483.844	74.743	OE 4
416723.3	5704818	-2491516.239	77.351	tread 4
416698.1	5704838	-2491547.607	77.811	IE 4
416693.1	5704841	-2491553.497	77.745	riser 4-5
416685	5704845	-2491562.932	80.416	OE 5
416576.3	5704881	-2491674.81	84.065	tread 5
416644.7	5705077	-2491713.492	89.53	tread 5
416604.8	5705236	-2491827.828	97.131	tread 5
416572.6	5705257	-2491866.173	99.152	riser 5- 6
416507.9	5705273	-2491930.098	105.671	riser 5- 6
416448.2	5705278	-2491984.466	108.486	OE 6
416288.8	5705276	-2492121.264	114.522	tread 6
416117.5	5705345	-2492304.203	117.439	tread 6
415918.1	5705355	-2492482.028	115.849	IE 6
415889.6	5705356	-2492507.269	116.939	riser 6- 7
415833.9	5705345	-2492549.599	121.993	OE 7
415748.8	5705330	-2492616.156	129.19	tread 7
415374.9	5705191	-2492870.095	148.139	fork in trail
415146.9	5705360	-2493152.427	149.098	fork in trail 2
414780.5	5705744	-2493661.645	147.979	road - trail intrsctn

WB 8

Easting	Northing	Projection	Elevation	Description
418165.5	5704434	5149267.263	27.824	tread 2
418183.5	5704395	5149243.001	24.912	tread 2
418203.1	5704327	5149193.307	20.593	OE 2
418202.6	5704300	5149170.431	21.97	riser 2-1
418202.8	5704288	5149159.762	20.706	riser 2-1
418202.8	5704277	5149149.903	17.528	riser 2-1
418203.3	5704258	5149134.016	13.115	IE 1
418204.3	5704238	5149116.928	9.424	tread 1
418205.2	5704204	5149087.978	7.763	tread 1
418228.9	5704171	5149071.783	7.981	tread 1
418224.7	5704082	5148992.039	5.356	tread 0
418226.1	5703985	5148908.553	3.597	tread 0

WB 9

Easting	Northing	Projection	Elevation	Description
416345.3	5703797	4327594.184	32.109	top clay
416305	5703824	4327584.498	39.179	silty clay- rd
416284.6	5703829	4327574.142	41.921	sandy clay-rd
416253.3	5703836	4327556.524	42.974	strat column loctn
416175.5	5703859	4327517.913	56.888	top rd
416102.1	5703879	4327480.489	64.136	trail intrsctn
416185.4	5703905	4327557.22	54.043	riser
416273.7	5703932	4327639.144	53.237	start tread
416386.2	5703962	4327739.724	50.166	tread
416392.6	5704060	4327813.562	49.245	tread
416397.7	5704141	4327874.742	51.059	tread
416427	5704184	4327925.893	50.437	tread trail intrsctn
416431	5703485	4327433.772	1.812	high-high tide
415456.1	5703783	4326955.429	123.434	trail west fault-fine sand

416749.5	5704799	-2491483.844	74.743	OE 4
416723.3	5704818	-2491516.239	77.351	tread 4
416698.1	5704838	-2491547.607	77.811	IE 4
416693.1	5704841	-2491553.497	77.745	riser 4-5
416685	5704845	-2491562.932	80.416	OE 5
416576.3	5704881	-2491674.81	84.065	tread 5
416644.7	5705077	-2491713.492	89.53	tread 5
416604.8	5705236	-2491827.828	97.131	tread 5
416572.6	5705257	-2491866.173	99.152	riser 5- 6
416507.9	5705273	-2491930.098	105.671	riser 5- 6
416448.2	5705278	-2491984.466	108.486	OE 6
416288.8	5705276	-2492121.264	114.522	tread 6
416117.5	5705345	-2492304.203	117.439	tread 6
415918.1	5705355	-2492482.028	115.849	IE 6
415889.6	5705356	-2492507.269	116.939	riser 6- 7
415833.9	5705345	-2492549.599	121.993	OE 7
415748.8	5705330	-2492616.156	129.19	tread 7
415374.9	5705191	-2492870.095	148.139	fork in trail
415146.9	5705360	-2493152.427	149.098	fork in trail 2
414780.5	5705744	-2493661.645	147.979	road - trail intrsctn

WB 8

Easting	Northing	Projection	Elevation	Description
418165.5	5704434	5149267.263	27.824	tread 2
418183.5	5704395	5149243.001	24.912	tread 2
418203.1	5704327	5149193.307	20.593	OE 2
418202.6	5704300	5149170.431	21.97	riser 2-1
418202.8	5704288	5149159.762	20.706	riser 2-1
418202.8	5704277	5149149.903	17.528	riser 2-1
418203.3	5704258	5149134.016	13.115	IE 1
418204.3	5704238	5149116.928	9.424	tread 1
418205.2	5704204	5149087.978	7.763	tread 1
418228.9	5704171	5149071.783	7.981	tread 1
418224.7	5704082	5148992.039	5.356	tread 0
418226.1	5703985	5148908.553	3.597	tread 0

WB 9

Easting	Northing	Projection	Elevation	Description
416345.3	5703797	4327594.184	32.109	top clay
416305	5703824	4327584.498	39.179	silty clay- rd
416284.6	5703829	4327574.142	41.921	sandy clay-rd
416253.3	5703836	4327556.524	42.974	strat column loctn
416175.5	5703859	4327517.913	56.888	top rd
416102.1	5703879	4327480.489	64.136	trail intrsctn
416185.4	5703905	4327557.22	54.043	riser
416273.7	5703932	4327639.144	53.237	start tread
416386.2	5703962	4327739.724	50.166	tread
416392.6	5704060	4327813.562	49.245	tread
416397.7	5704141	4327874.742	51.059	tread
416427	5704184	4327925.893	50.437	tread trail intrsctn
416431	5703485	4327433.772	1.812	high-high tide
415456.1	5703783	4326955.429	123.434	trail west fault-fine sand

WB 10

Easting	Northing	Projection	Elevation	Description
419243.6	5703856	5690002.061	6.052	OE 1
419164	5703961	5690091.729	7.485	tread 1
419033.3	5704079	5690185.882	10.627	tread 1
418998.5	5704120	5690219.762	10.273	tread 1
419050.1	5704219	5690326.207	14.136	tread 1
419027.6	5704345	5690446.252	15.438	IE 1
419013.8	5704391	5690488.996	14.352	riser
419009.7	5704429	5690526.058	18.94	OE 2
419001.1	5704541	5690635.343	19.088	tread 2
418801.5	5704856	5690910.76	25.294	tread 2
418503.9	5705199	5691196.476	31.467	tread 2
418234	5705473	5691419.823	38.787	tread 2
417813.4	5705746	5691615.899	48.476	tread 2
417667.8	5706000	5691839.84	57.008	IE 2
417637.3	5706033	5691867.126	60.842	riser
417608.7	5706069	5691897.809	64.613	OE 3
417567.6	5706338	5692156.01	73.729	tread 3
417570.9	5706401	5692217.959	77.948	IE 3
417570.8	5706413	5692230.209	79.401	riser
417572.6	5706445	5692262.058	81.891	OE 4
417575.4	5706500	5692316.666	84.348	tread 4
417577.2	5706565	5692380.786	86.841	tread 4
417579.2	5706614	5692429.818	92.253	IE 4
417581.5	5706653	5692468.549	98.915	riser
417584.9	5706725	5692540.099	107.724	OE 5
420585.8	5705256	5691614.468	23.011	hhgravel-roadcut

Appendix B: Alternative Sea Level Curve Correlations

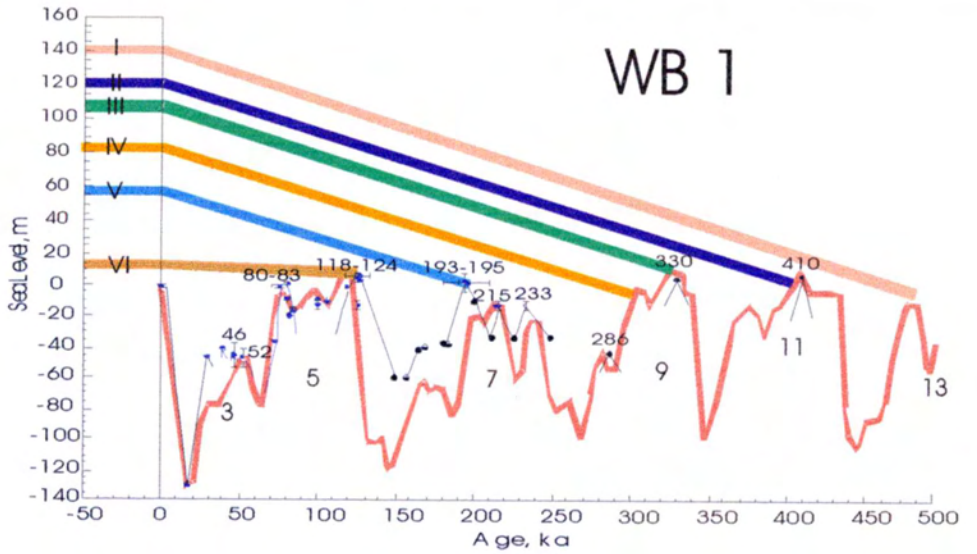

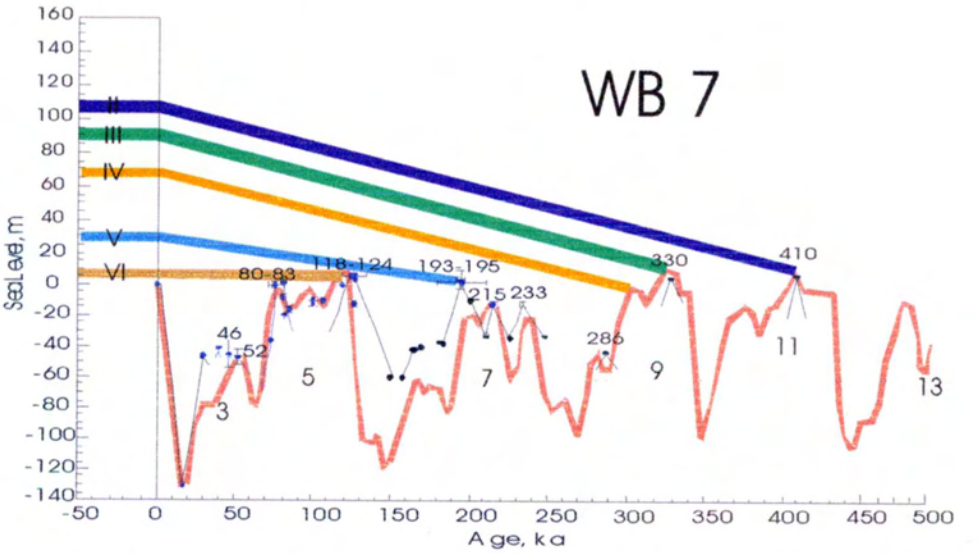

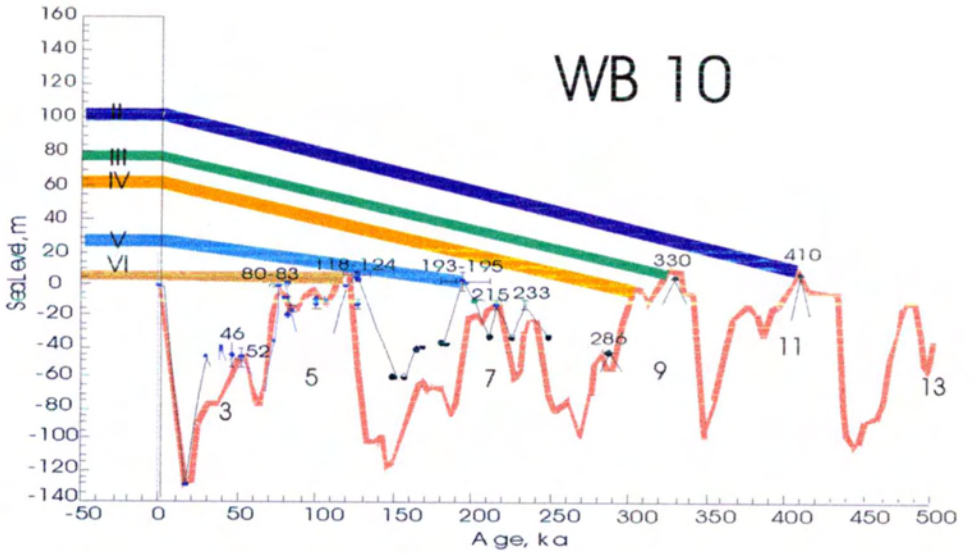

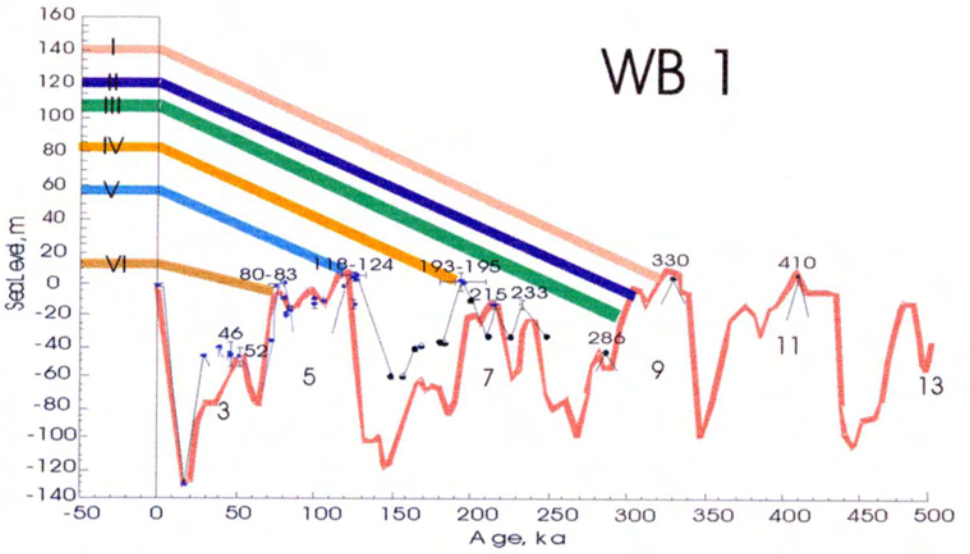
WB 1
Sea Level, m
Age, ka
I
II
III
IV
V
VI
80-83
118-124
193-195
215
233
46
52
286
330
410
3
5
7
9
11
13

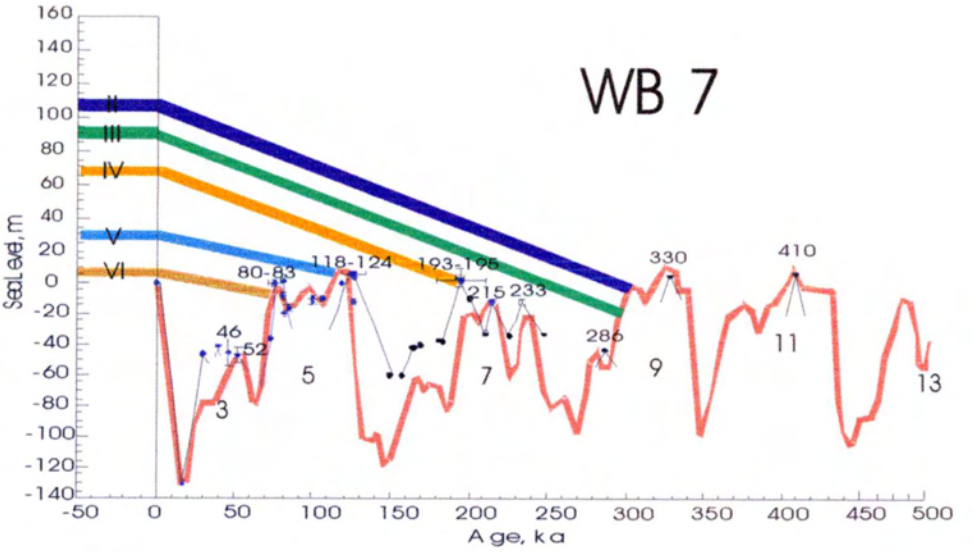
WB 7
Sea Level, m
Age, ka
II
III
IV
V
VI
80-83
118-124
193-195
215
233
46
52
286
330
410
3
5
7
9
11
13

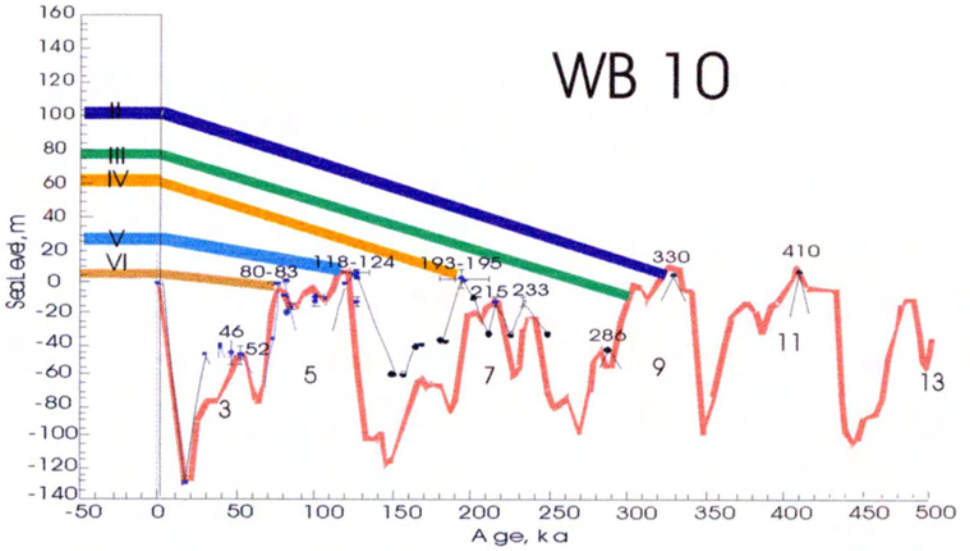
WB 10
Sea Level, m
Age, ka
II
III
IV
V
VI
80-83
118-124
193-195
215
233
46
52
286
330
410
3
5
7
9
11
13

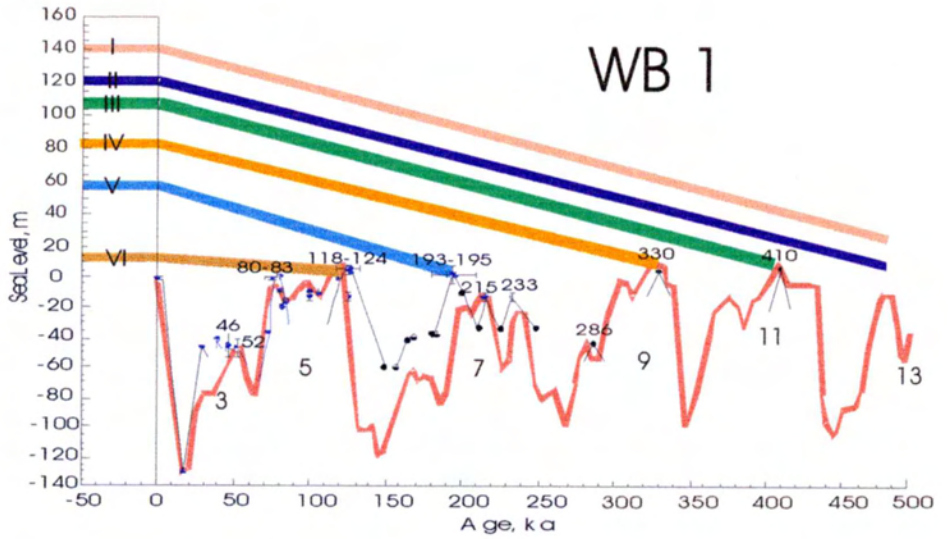
WB 1
Sea Level, m
Age, ka
I
II
III
IV
V
VI
80-83
118-124
193-195
215
233
46
52
330
410
286
3
5
7
9
11
13

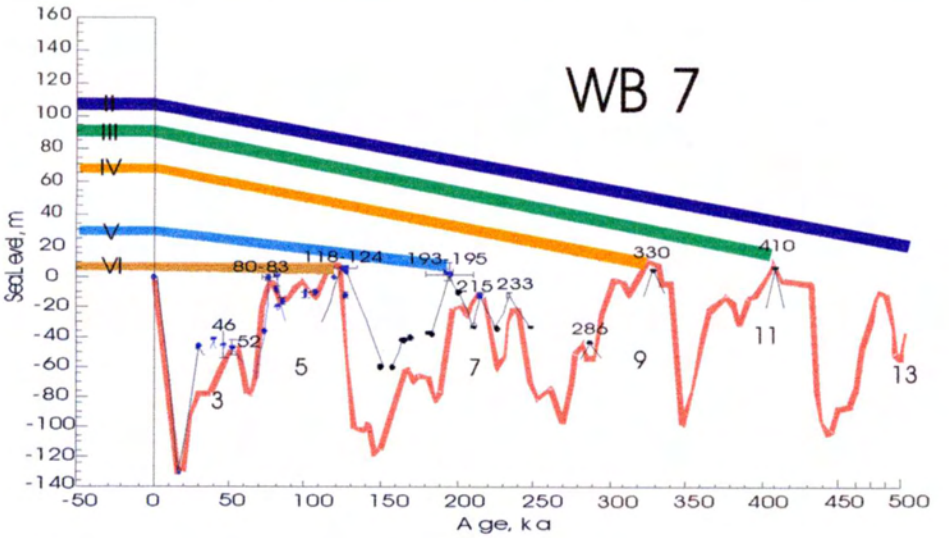
WB 7
Sea Level, m
Age, ka
II
III
IV
V
VI
80-83
118-124
193-195
215
233
46
52
330
410
286
3
5
7
9
11
13

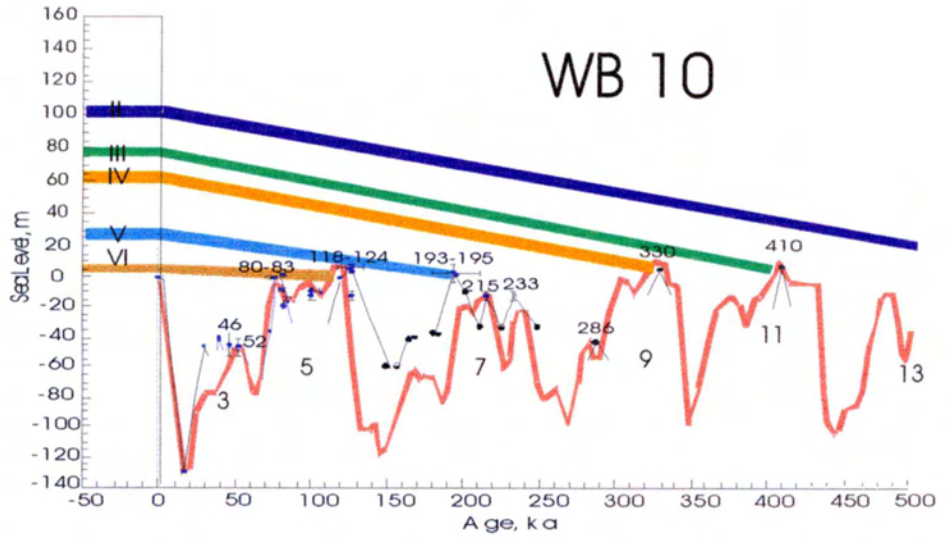
WB 10
Sea Level, m
Age, ka
II
III
IV
V
VI
80-83
118-124
193-195
215
233
46
52
330
410
286
3
5
7
9
11
13